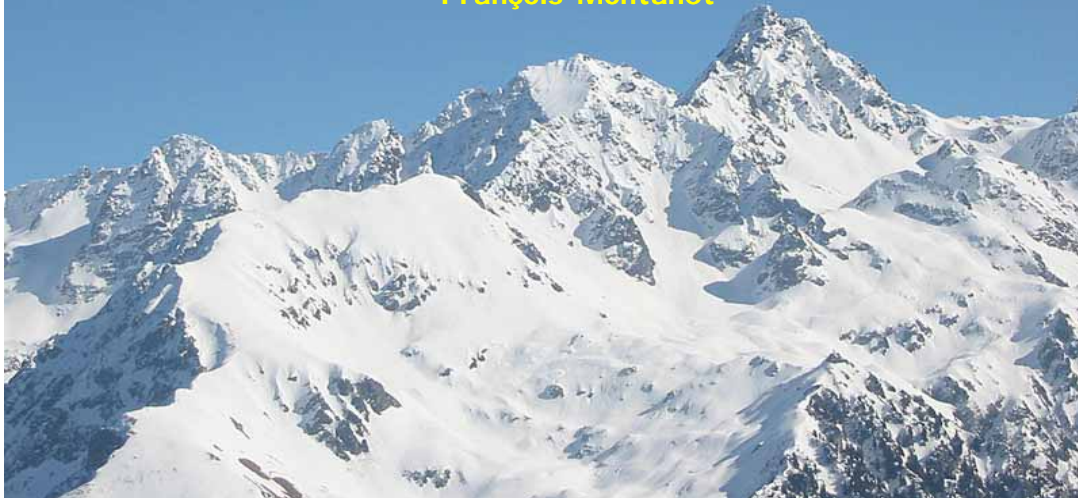


Cherenkov and Imaging detectors for HEP and AP

ESIPAP - 2014
François Montanet



2014

F. Montanet Experimental Astroparticle Physics ESIPAP

- The Cherenkov effect, theory and phenomenology
- Timing and counting particles
 - The AUGER WCD as an example
- Identifying particles
 - Threshold Cherenkov counters
 - NA9, BELLE
 - Ring Imaging Cherenkov detectors (RICH, DIRC)
 - DELPHI, LHCb, BaBar
 - Measuring charge
 - AMS, CREAM
- VHE gamma rays
 - HESS, MAGIC, VERITAS...
- Neutrino detectors
 - SK, Amanda, Antares, Icecube

2

THE CHERENKOV EFFECT



2014

F. Montanet Experimental Astroparticle Physics ESIPAP

Comptes Rendus (Dokl.) Acad. Sci. URSS 14, 109-114 (1937)

Comptes Rendus (Doklady) de l'Académie des Sciences de l'URSS
1937, Volume XIV, No 3

PHYSICS

COHERENT VISIBLE RADIATION OF FAST ELECTRONS PASSING THROUGH MATTER

By I. FRANK and Ig. TAMM, Corresponding Member of the Academy

In 1934 P. A. Cherenkov has discovered a peculiar phenomenon, which he has since investigated in detail^(*). All liquids and solids if bombarded by fast electrons, such as β -electrons or Compton electrons produced by γ -rays, do emit a peculiar visible radiation, quite different from the eventual ordinary fluorescence. This radiation is partially polarized, the electric oscillation vector being parallel to the electron beam, and its intensity can be reduced neither by temperature nor by addition to the liquid bombarded of quenching substances. The peculiarity of these characteristics was scrutinized by Wawilow^(*) who suggested that this radiation must be connected with the «Bremsung» of fast electrons. Since then a new and undoubtedly the most peculiar characteristic of the phenomenon was discovered, namely, its highly pronounced asymmetry, the intensity of light emitted in the direction of the motion of electrons being many times larger than in the backward direction. It follows that the substance bombarded radiates coherently for the space of at least one wavelength of the visible light.

This peculiar radiation can evidently not be explained by any common mechanism such as the interaction of the fast electron with individual atom or as radiative scattering of electrons on atomic nuclei.* On the other hand, the phenomenon can be explained both qualitatively and quantitatively if one takes in account the fact that an electron moving in a medium does radiate light even if it is moving uniformly provided that its velocity is greater than the velocity of light in the medium.

We shall consider an electron moving with constant velocity v along the z axis through a medium characterized by its index of refraction n . The field of the electron may be considered as the result of superposition of spherical waves of retarded potential, which are being continually emitted by the moving electron and are propagated with the velocity $\frac{c}{n}$. It is easy to see that all these consecutive waves emitted

* The intensity of visible light emitted by the last named process is about 10^4 times smaller than the intensity observed.

Plan of the course

The Nobel Prize in Physics 1958
Pavel A. Cherenkov, Il'ja M. Frank, Igor Y. Tamm

The Nobel Prize in Physics 1958



Pavel Alekseyevich Cherenkov



Il'ja Mikhailovich Frank



Igor Yevgenyevich Tamm

The Nobel Prize in Physics 1958 was awarded jointly to Pavel Alekseyevich Cherenkov, Il'ja Mikhailovich Frank and Igor Yevgenyevich Tamm "for the discovery and the interpretation of the Cherenkov effect".

Photos: Copyright © The Nobel Foundation

4

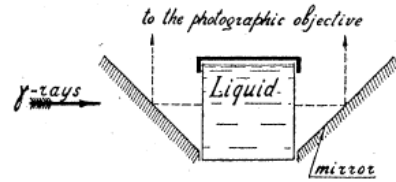


FIG. 1. Arrangement of apparatus.

All the results obtained are in good agreement with I. M. Frank and I. E. Tamm's theory of the coherent radiation of electrons moving in a medium.⁶

P. A. ČERENKOV

The Physical Institute of the Academy of Sciences of U.S.S.R.,
Moscow,
June 15, 1937.

¹ Čerenkov, C. R. Ac. Sci. U.S.S.R. 8, 451 (1934).

² Čerenkov, C. R. Ac. Sci. U.S.S.R. 12 (3), 413 (1936).

³ Čerenkov, C. R. Ac. Sci. U.S.S.R. 14, 102 (1937).

⁴ Čerenkov, C. R. Ac. Sci. U.S.S.R. 14, 105 (1937).

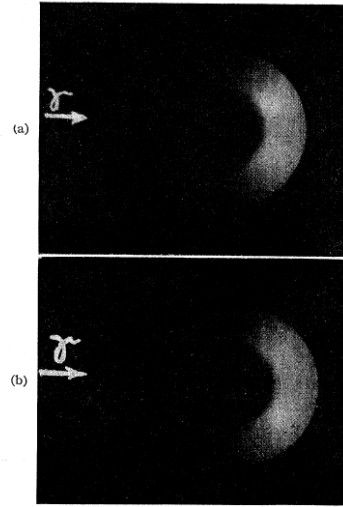
⁵ Wawilow, C. R. Ac. Sci. U.S.S.R. 8, 457 (1934).

⁶ Frank and Tamm, C. R. Ac. Sci. U.S.S.R. 14, 109 (1937).

⁷ Bull. Ac. Sci. U.S.S.R., No. 7, 919 (1933).

⁸ E. Brumberg and S. Wawilow, C. R. Ac. Sci. U.S.S.R. 3, 405 (1934)

FIG. 2. Photographs showing asymmetry of luminescence. (a) water, $n = 1.337$; (b) benzene, $n = 1.513$.

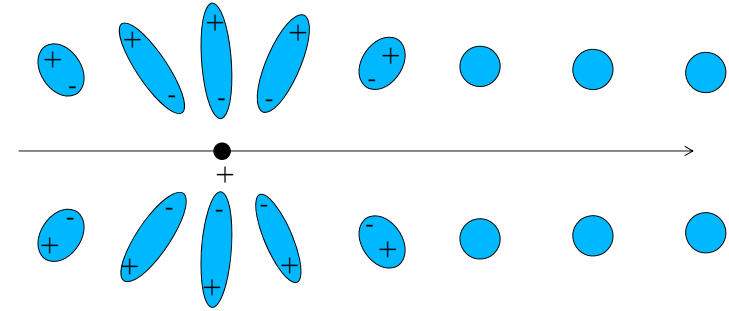


P.A. Čerenkov Letter to the editor Phys.Rev 53 (1937) 378

5

Theory of the Cherenkov effect

- Dielectric medium electrons polarized by a moving charged particle.



- De-excitation give rise to a coherent radiation.
- Same basic process as energy loss (Bethe, Fermi).

6

The Cherenkov effect

- When a charged particle moves faster than the phase speed of light in a medium, electrons interacting with the particle can emit coherent photons while conserving energy and momentum.
- This process can be viewed as a decay.
- It is actually not the particle that emits light, but the bounded (dielectric) electrons of the immediately surrounding medium.
- Emission is coherent because in phase with the particle velocity.
- Pavel A. Čerenkov and Vavilov discovered the radiation in 1934, Igor Tamm and Ilya Frank explained it in 1937.

7

The theory of the Cherenkov effect

Ig. Tamm and Il. Frank

The energy emitted per unit length dx travelled by the particle per unit of angular frequency $d\omega$ is:

$$dE = \frac{q^2}{4\pi} \mu(\omega) \omega \left(1 - \frac{c^2}{v^2 n^2(\omega)} \right) dx d\omega$$

provided that $\beta = \frac{v}{c} > \frac{1}{n(\omega)}$. Here $\mu(\omega)$ and $n(\omega)$ are the frequency-dependent permeability and index of refraction of the medium, q is the electric charge of the particle, v is the speed of the particle, and c is the speed of light in vacuum.

Consequences:

- the **yield** of photons is **flat** versus these photons energy ($h\nu$).
- the **yield** of photons is $\propto \lambda^{-2} \Rightarrow$ prominent at small wavelengths (UV)
- the spectrum is continuous \neq fluorescence

8

The Cherenkov effect

The total amount of energy radiated per unit length is:

$$\frac{dE}{dx} = \frac{q^2}{4\pi} \int_{v > \frac{c}{n(\omega)}} \mu(\omega) \omega \left(1 - \frac{c^2}{v^2 n^2(\omega)} \right) d\omega$$

This integral is done over the frequencies ω for which the particle's speed v is greater than speed of light of the media $\frac{c}{n(\omega)}$. The integral is non-divergent because at high frequencies the refractive index becomes less than unity.

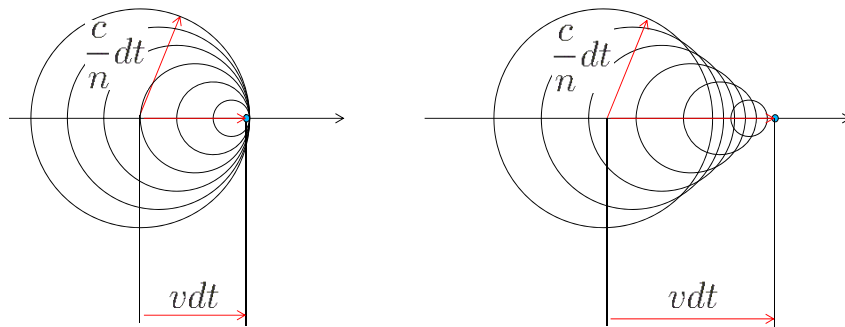
$$\frac{dE}{dx} = \frac{q^2}{4\pi} \int_{v > \frac{c}{n(\omega)}} \mu(\omega) \omega \left(1 - \frac{1}{\beta^2 n^2(\omega)} \right) d\omega$$

The Cherenkov effect

- Cerenkov radiation consist of a shock wave
- Similar to Doppler effect or Mach shock waves

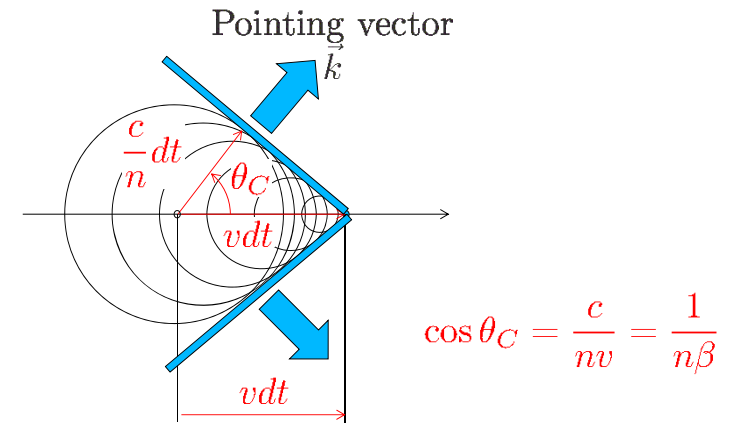
The Cherenkov effect

- Cerenkov radiation consist of a shock wave
- Similar to Doppler effect or Mach shock waves



The Cherenkov effect

- Cerenkov radiation consist of a shock wave
- Similar to Dopler effect or Mach shock waves



Cherenkov effect

- Relevant formulae:

The emission angle wrt particle direction:

$$\theta_C = \arccos\left(\frac{1}{n\beta}\right)$$

if $n\beta > 1$.

The threshold velocity:

$$\beta_{th} = \frac{1}{n}$$

thus the threshold momentum:

$$p_{th} = m\beta_{th}\gamma_{th} = \frac{m}{\sqrt{n^2 - 1}} \approx \frac{m}{\sqrt{2\delta}}$$

with $\delta = n - 1 \ll 1$

13

Cherenkov effect

- Relevant formulae:

The number of photons produced per unit length and unit of photon energy by a particle with charge Ze :

$$\begin{aligned} \frac{d^2 N}{dE dx} &= \frac{\alpha Z^2}{\hbar c} \sin^2 \theta_C \\ &= \frac{\alpha Z^2}{\hbar c} \left(1 - \frac{1}{\beta^2 n^2(E)}\right) \\ &= 370 Z^2 \sin^2 \theta_C \text{eV}^{-1} \text{cm}^{-1} \end{aligned}$$

or equivalently:

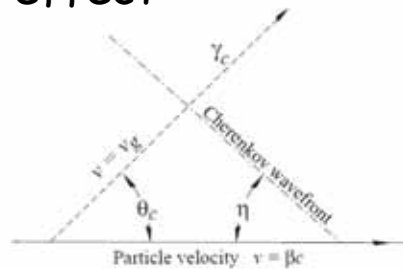
$$\frac{d^2 N}{d\lambda dx} = \frac{2\pi\alpha Z^2}{\lambda^2} \sin^2 \theta_C$$

14

Cherenkov effect

- Dispersive material:

Important for timing of neutrino telescopes



In dispersive media (where $dn/d\omega \neq 0$) one has to take into account the fact that photons propagate with the **group** velocity. Tamm showed that in that case $\theta_C + \eta \neq 90^\circ$ with η the cone 1/2 opening angle given by:

$$\begin{aligned} \cot \eta &= \left[\frac{d}{d\omega} (\omega \tan \theta_C) \right]_{\omega_0} \\ &= \left[\tan \theta_C + \beta^2 \omega n(\omega) \frac{dn}{d\omega} \cot \theta_C \right]_{\omega_0} \end{aligned}$$

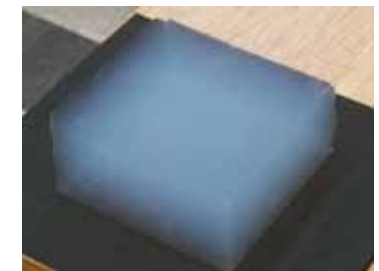
15

Radiators

- Adapt refractive index to the momentum range.

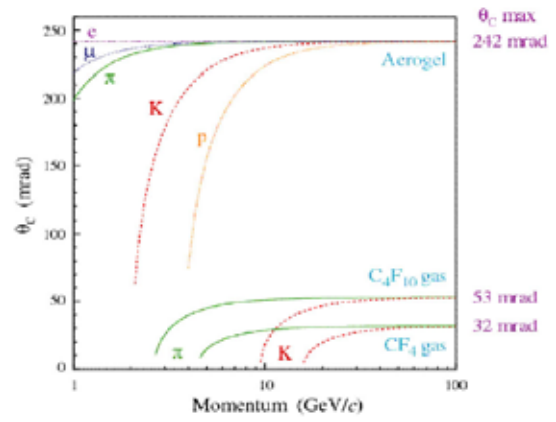
Medium	$n - 1$	γ_{th}	θ_C	Photons/m
He (stp)	$3.5 \cdot 10^{-5}$	120	0.48°	3
C ₂ (stp)	$4.1 \cdot 10^{-4}$	35	1.64°	40
Silica aerogel	0.025 – 0.075	4.6 – 2.7	$12.7 - 21.5^\circ$	2400 – 6600
Water	0.33	1.52	41.2°	$2.1 \cdot 10^4$
Glass	0.46 – 0.75	1.37 – 1.22	$46.8 - 55.1^\circ$	$2.6 - 3.3 \cdot 10^4$

Silica aerogel:
SiO₂ "foam" with
nano-size structure $\ll \lambda$



16

Cherenkov angle vs mass and momentum

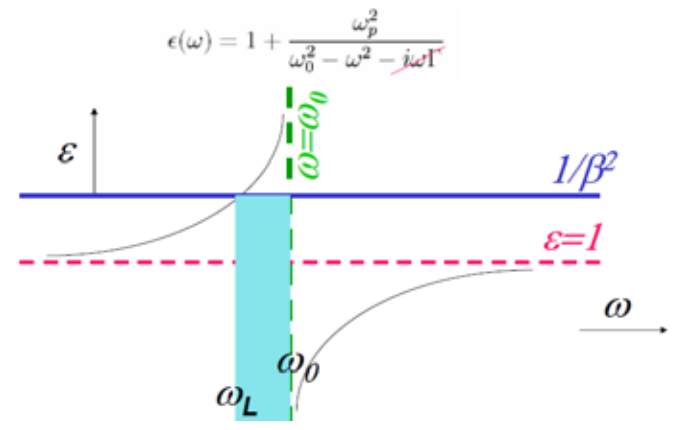


$$\cos \theta_C = \frac{c}{nv} = \frac{1}{n\beta}$$

2014 F. Montanet Experimental Astroparticle Physics ESIPAP

Dielectrics

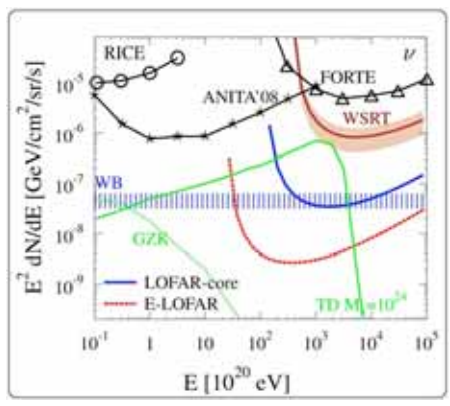
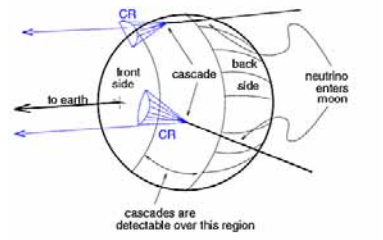
- Simple model for dielectric materials



2014 F. Montanet Experimental Astroparticle Physics ESIPAP

Cherenkov not only optical

- Radio-wave Cherenkov emission (also called Askarian effect) by EM showers in dense dielectric materials (ice, salt, sand, lunar regolith ...)
- Coherent Cherenkov like emission for $\lambda \gg$ shower size $\approx X_0$



2014 F. Montanet Experimental Astroparticle Physics ESIPAP

TIMING AND COUNTING: THE AUGER DETECTOR EXAMPLE

2014 F. Montanet Experimental Astroparticle Physics ESIPAP

Counting particles or timing measurements

- Example : the Auger Water Cherenkov Tanks

2014 F. Montanet Experimental Astroparticle Physics ESIPAP



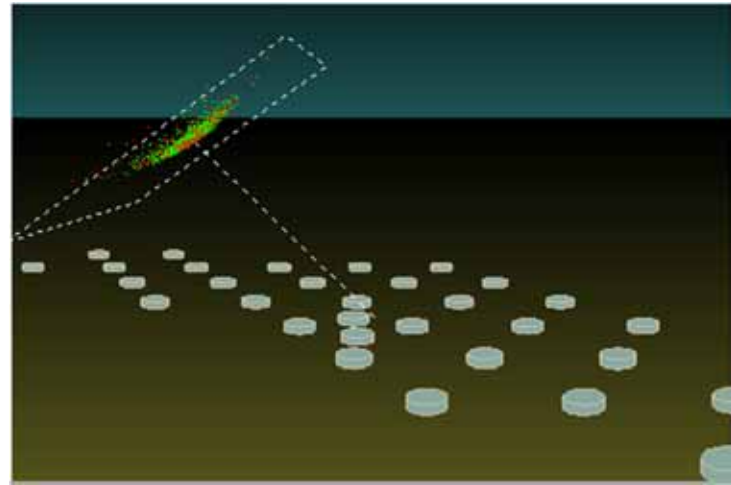
L'Observatoire Pierre Auger

2014 F. Montanet Experimental Astroparticle Physics ESIPAP



Timing

2014 F. Montanet Experimental Astroparticle Physics ESIPAP

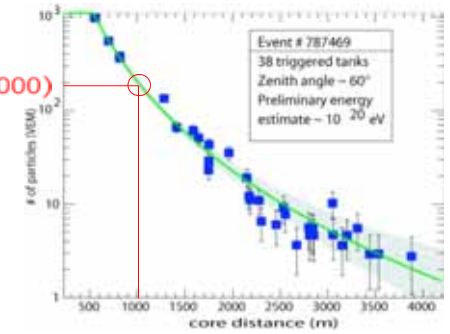
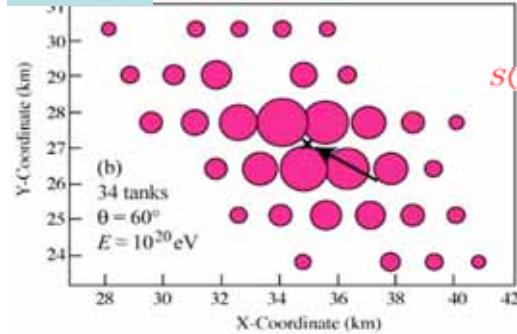


Thin pancake (few tens ns) of particles traveling at speed $v \sim c$. Spacing is 1.5 km \Rightarrow few 10 ns relative timing to achieve 0.1° angular resolution for vertical showers. Achievable with GPS + flash ADCs.

From EAS footprint and LDF to primary CR energy estimator

2014 F. Montanet Experimental Astroparticle Physics ESIPAP

AUGER



- Idea from Hillas 1970 (pioneered by Haverah Park and Agasa)
 - energy estimator: signal @ fixed (large) core distance $S(R)$
 - small shower-to-shower fluctuations, depends on primary E only
 - Determination of particle density \rightarrow LDF $\rightarrow S(R)$
 - Largest uncertainty: converting estimator to energy (see later)

The surface array detectors

2014 F. Montanet Experimental Astroparticule Physique ESPAP

Communication antenna

GPS

Electronics 40 MHz FADC

Solar panel

Light diffusing inner liner

3 PMTs

Plastic tank 12 tons of water

Batteries

Radio waves

Central DAQ

Local trigger

Trigger Seuil

Coups d'ADC

Temps (25ns/bin)

Coincidence 3 PMT > 1.75 VEM

Trigger TOI

Coups d'ADC

Temps (25ns/bin)

Coincidence 2 PMT > 0.2 VEM sur 13 bins sur une periode de 120 bins de 2ns

Self-calibration:
1 VEM = average signal from vertical through going muons.

Installing the world largest particle detector

2014 F. Montanet Experimental Astroparticule Physique ESPAP

~20

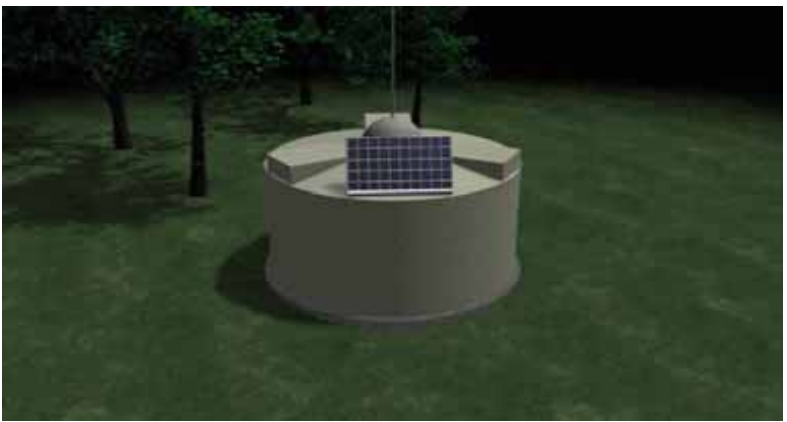
Installing electronics

Moving to

W

Pierre Auger Observatory surface detectors

2014 F. Montanet Experimental Astroparticule Physique ESPAP



An UHECR event

2014 F. Montanet Experimental Astroparticule Physique ESPAP

Generic Information

Id / Date	10485600 / Tue Oct 26 17:39:16 2010
Nb. of stations	14
Energy	49.7 ± 1.9 EeV
Theta	40.2 ± 0.2 deg
Phi	-139.2 ± 0.5 deg
Curvature	10.9 ± 0.5 km
Core Easting	476053 ± 19 m
Core Northing	6079248 ± 12 m
Reduced Chi ²	8.36

Signal (VEM)

Distance to axis (m)

Log(Signal) (VEM)

Time (ns)

Time (ns)

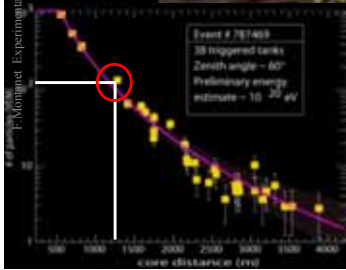
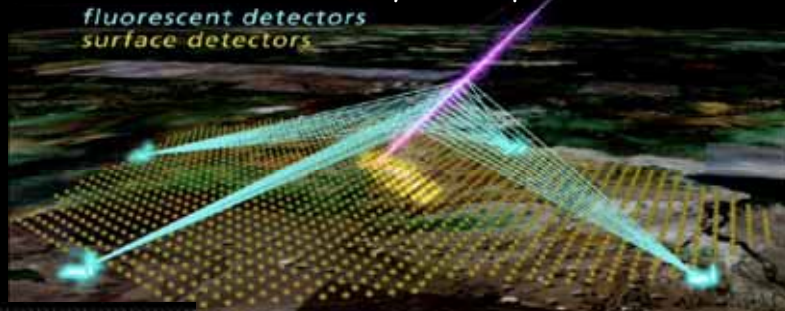
PMT 1

PMT 2

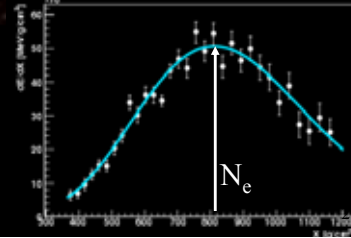
PMT 3

From EAS longitudinal profile to primary CR energy

The Hybrid "image" of the same shower, pioneered by Auger, increases as well the accuracy of the profile measurement.



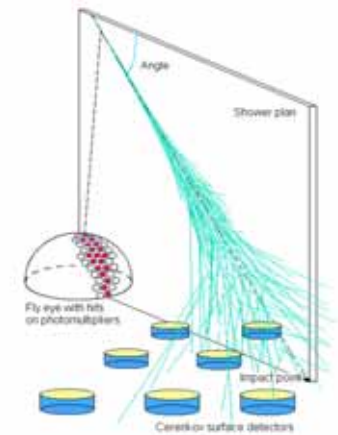
PROGRESS:
Calibration of SD energy estimator through FD



Improving measurements

Fluorescence vs Hybrid techniques :

	Hybrid	SD only	FD only
Angular resolution	0.2°	1-2°	3-5° (0.5° stereo)
Aperture	Independent on E, mass, models.	Independent on E, mass, models.	Dependent on E, mass, models, spectral shape.
Energy	Independent on mass, models.	Dependent on mass, models.	Independent on mass, models.



F.Montanet Experimental Astroparticle Physics ESPAP

2014

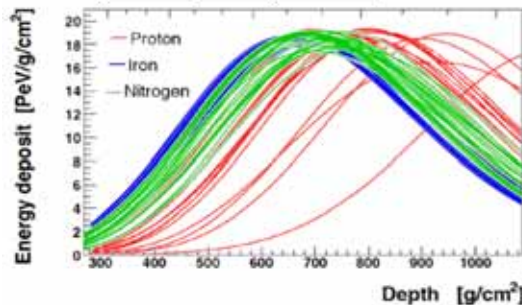
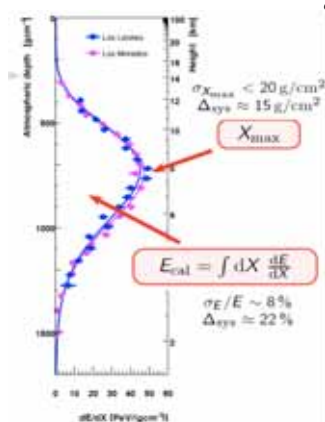
30

From EAS longitudinal profile to primary CR mass composition

Average depth of shower maximum $\langle X_{max} \rangle$:

Width of distribution $RMS(X_{max})$ at a certain E

sensitive to primary composition



$$X_{max} \propto \ln(E_0) - \ln(A) \text{ (MC Sim.)}$$

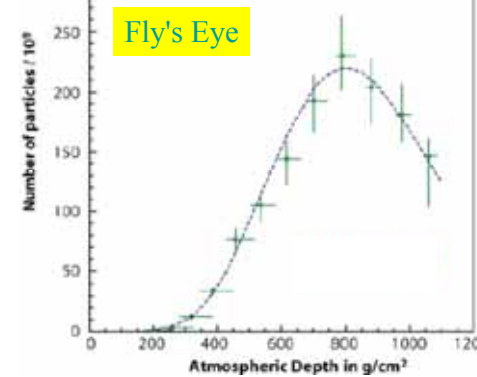
2014

F.Montanet Experimental Astroparticle Physics ESPAP

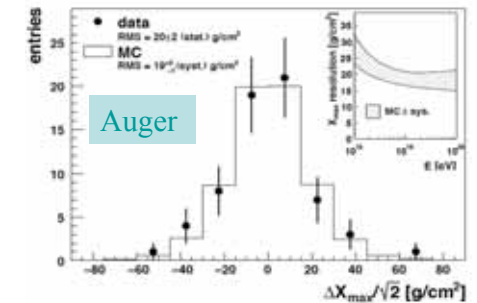
31

From EAS longitudinal profile to primary CR mass

$\sigma(X_{max}) \approx 60 \text{ g/cm}^2$



$\sigma(X_{max}) \approx 20 \text{ g/cm}^2$



PROGRESS:

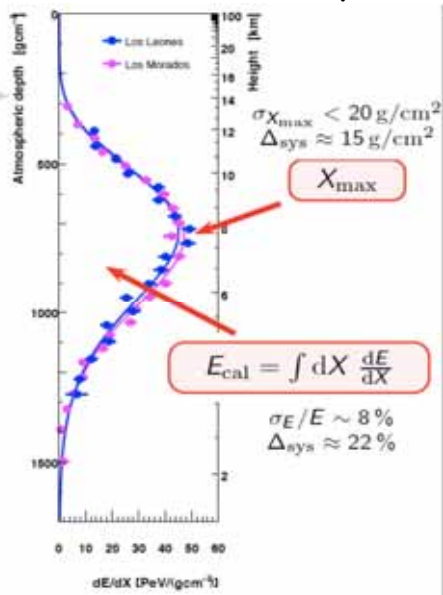
Fly's Eye showed experimental access to X_{max} through fluorescence
High precision now possible through higher resolution + stereo and hybrid measurements (around 20-25 g/cm²) N.B. : $\langle X_{max} \rangle_{proton} - \langle X_{max} \rangle_{iron} \approx 150 \text{ g/cm}^2$
Delicate issues: great care in event selection (possible biases)
Important drawback: strong need for models in the interpretation

2014

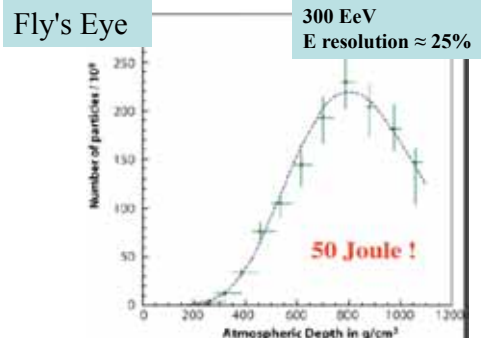
F.Montanet Experimental Astroparticle Physics ESPAP

32

From EAS longitudinal profile to primary CR energy



- PROGRESS:
- Calorimetric measurement of E with :
 - Fluorescence technique
 - Validated by Fly's Eye
 - Largest uncertainty: fluorescence yield,
 - Atmosphere, "missing" energy
 - No hadronic model dependence



FD at 4 sites:
each 6 telescopes 30°x30° field of view each

440 PMTs / telescope 1.4°x1.4° pixels
(Photonis XP 3062)

Pierre Auger Observatory fluorescence detectors



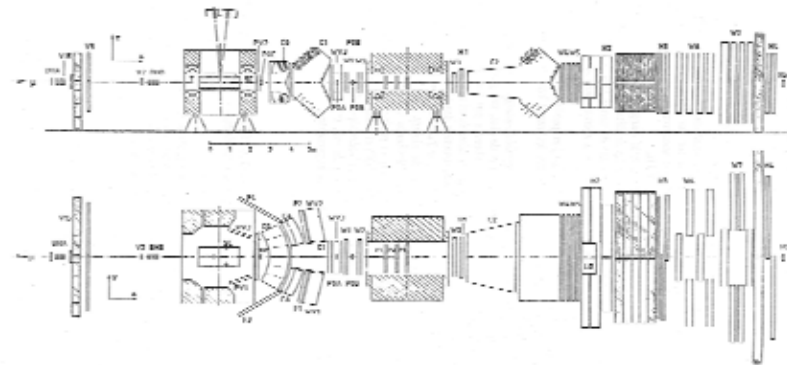
Pierre Auger Observatory fluorescence detectors



IDENTIFYING PARTICLES MEASURING PARTICLE VELOCITY

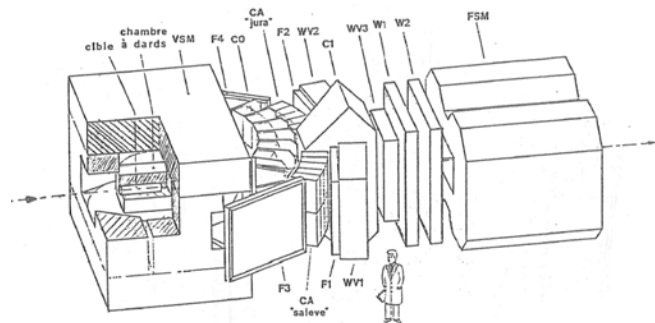
Threshold Cherenkov counters

- Hundredth of examples on fix target experiments, where different threshold cherenkov can be used to separate particle masses over a large range of momentum and over large solid angles.
- for example NA9:



Threshold Cherenkov

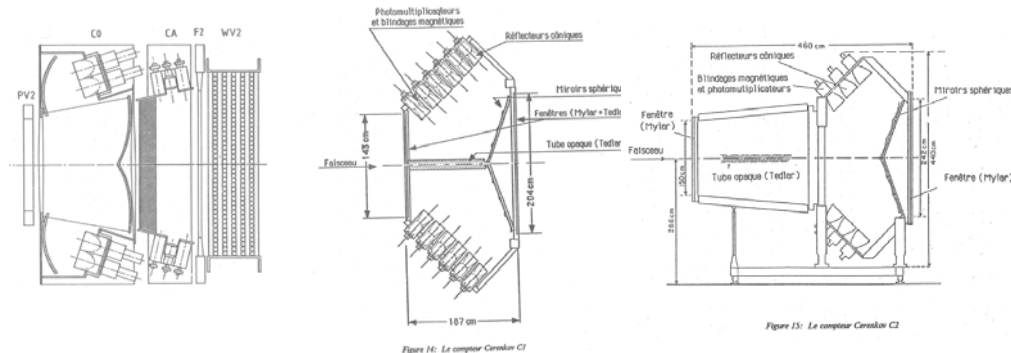
- NA9:



Detecteur	Couverture angulaire horizontale	Zone sensible (cm ²)	Taille des cellules	Radiateur n-1= (valeurs approximatives)	Valeurs des seuils $\pi/K/p$ (Gev/c)
F1,F2 F3,F4	$\pm(10-34)^\circ$ $\pm(32-60)^\circ$	160x 106 160x252	160x 10 160x 15	NE 110 NE 110	$\pi/K < 1,5$ $K/P < 2,5$
CA	$\pm(10-32)^\circ$	2x 150x 130	65x 30	acrogel 0,030	0,6/2/3,8
C0	$\pm 32^\circ$	2x 300x 100	12x 14 25x 28	néopentane 0,0015	2,6/9,1/17
C1	$\pm 9^\circ$	109x 143	14x 18	azote 3×10^{-4}	5,6/20/38
C2	$\pm 7^\circ$	150x 300	23x 25	néon 6×10^{-5}	12/42/79

Threshold Cherenkov

- NA9:



Threshold Cherenkov

- NA9:

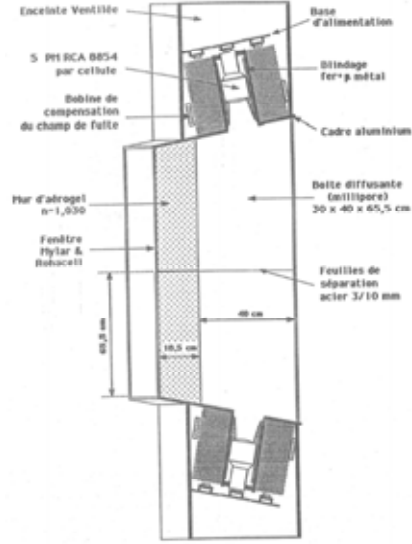
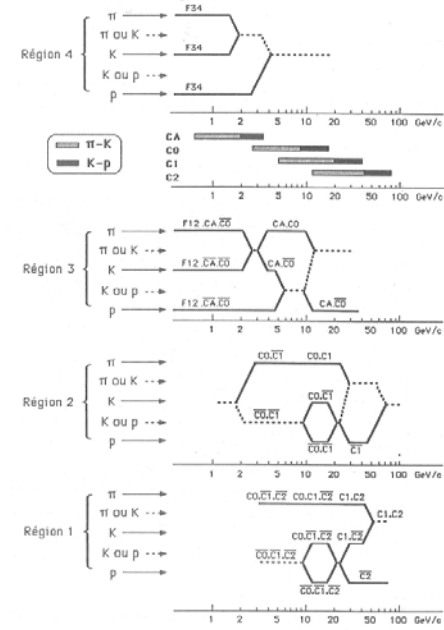


Figure 35. Vue en coupe du compteur Cherenkov à aérogel

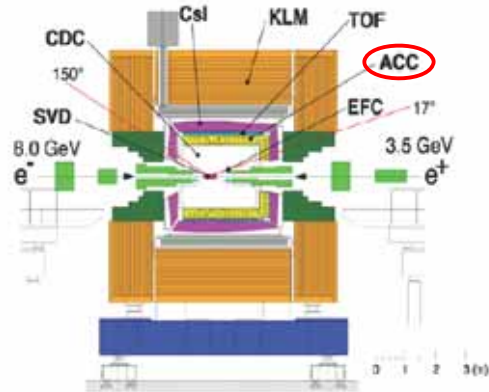
Threshold Cherenkov

- NA9:



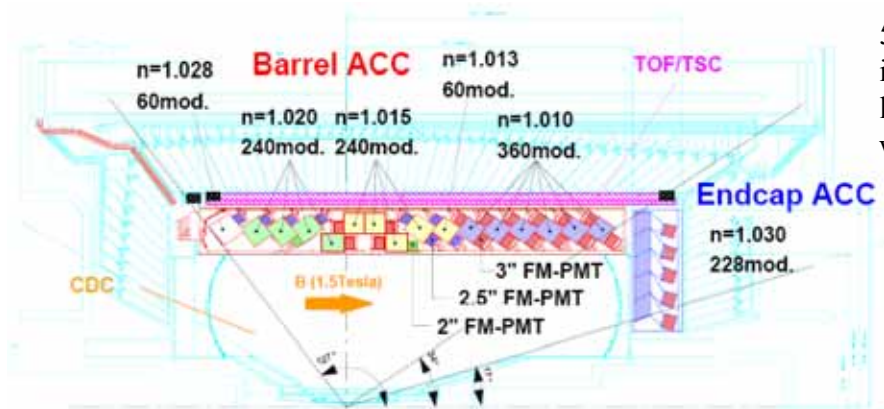
Threshold detectors

- A more recent example BELLE at KEKB
- CP violation in B mesons at e+e- collider.
- Current design: threshold aerogel Cherenkov counters to help discriminate pi from K



Threshold detectors

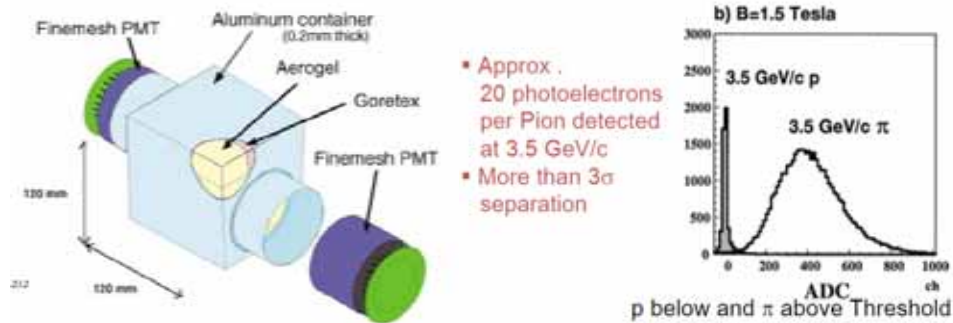
- A more recent example BELLE at KEKB



5 aerogel tiles inside a boxed lined with white reflector

Threshold detectors

- A more recent example BELLE at KEKB

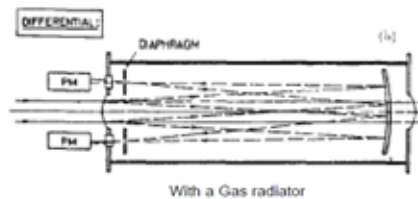


- Approx. 20 photoelectrons per Pion detected at 3.5 GeV/c
- More than 3σ separation

IDENTIFYING PARTICLES MEASURING THE CHERENKOV ANGLE: DIFFERENTIAL, RICH, DIRC,

Differential Cherenkov Counters

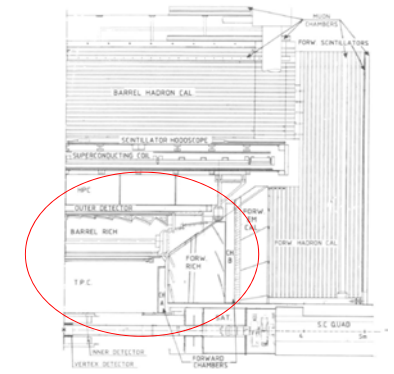
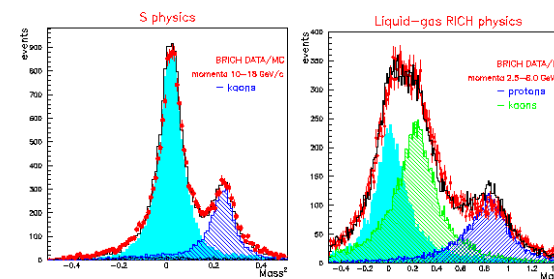
- Used along beam lines to discriminate masses.
- Mesons beams (π^\pm , K^\pm), hyperon beams etc...
- Example: CEDAR at CERN



		CEDAR - W	CEDAR - N
Velocity resolution	$\Delta\beta$	$5 \cdot 10^{-6}$	10^{-6}
Radiator	gas	N_2	He
	length L	5.8 m	5.8 m
	pressure P	1.6 - 8 bar	10 - 14 bar
	C angle θ	30.8 mrad	25.8 mrad

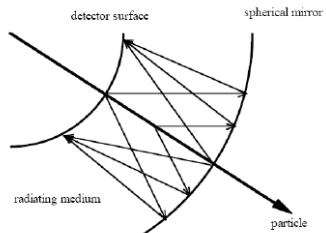
RICH detectors

- Ring Imaging Cherenkov detectors
- First used on a fix target experiment, the OMEGA spectrometer at CERN (J. Séguinot & T. Ypsilantis)
- Major breakthrough with the DELPHI RICH
- Liquid and gas fluorocarbon radiators (2 detectors in //)
- Optimized for $\pi / K / p$ separation up to 30 GeV/c



RICH detectors

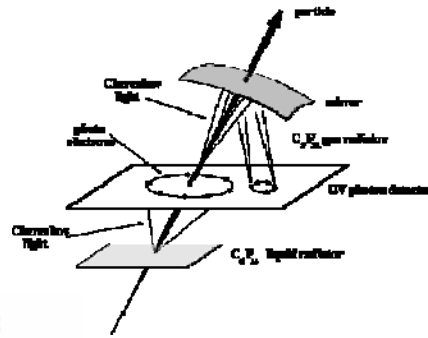
- Ring Imaging Cherenkov detectors: measure both θ_C and N_{ph}



$$\frac{\Delta\beta}{\beta} = \tan(\theta) \Delta\theta_C$$

where $\Delta\theta_C = \langle \Delta\theta_C \rangle / \sqrt{N_{ph}} + C$

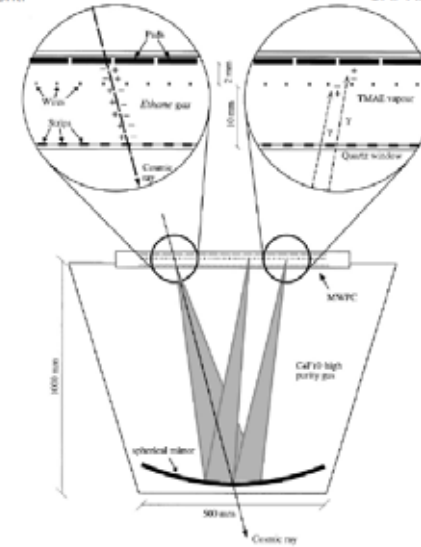
For 1.4m long CF_4 gas radiator at stp and $N_0 = 75cm^{-1}$,
 $\frac{\Delta\beta}{\beta} = 1.6 \cdot 10^{-6}$



RICH also for astroparticles

Balloon Experiment:
RICH detector

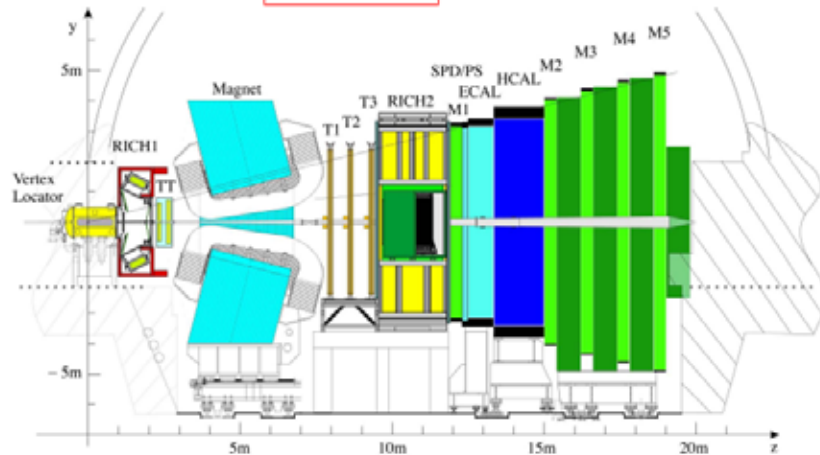
CAPRICE Experiment



TMAE:
(tetrakis(dimethylamino)
ethylene)

LHCb RICH

LHCb Experiment



- Precision measurement of B-Decays and search for signals beyond standard model.
- Two RICH detectors covering the particle momentum range $1 \rightarrow 100$ GeV/c using aerogel, C_4F_{10} and CF_4 gas radiators.

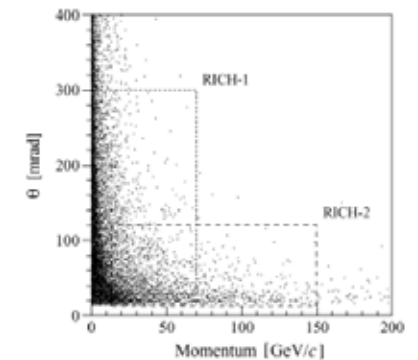
LHCb RICH

LHCb-RICH Design

RICH1: Aerogel $L=5cm$ $p: 2 \rightarrow 10$ GeV/c
 $n=1.03$ (nominal at 540 nm)
 C_4F_{10} $L=85$ cm $p: < 70$ GeV/c
 $n=1.0014$ (nominal at 400 nm)

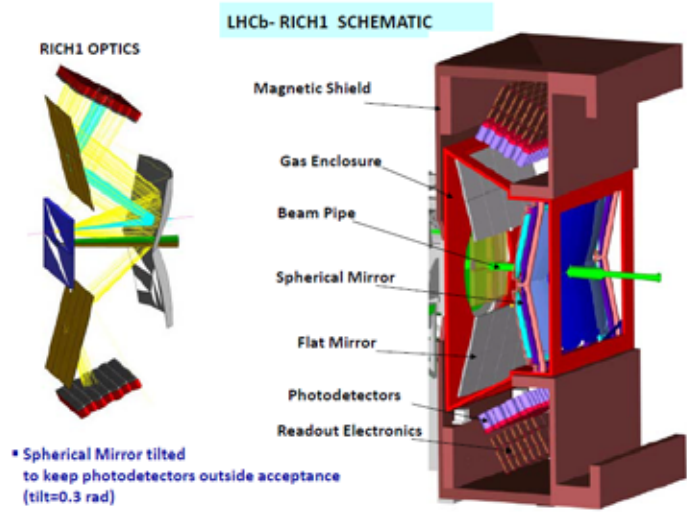
Upstream of LHCb Magnet
 Acceptance: $25 \rightarrow 250$ mrad (vertical)
 300 mrad (horizontal)
 Gas vessel: $2 \times 3 \times 1$ m³

RICH2: CF_4 $L=196$ cm $p: < 100$ GeV/c
 $n=1.0005$ (nominal at 400 nm)
 Downstream of LHCb Magnet
 Acceptance: $15 \rightarrow 100$ mrad (vertical)
 120 mrad (horizontal)
 Gas vessel : 100 m³



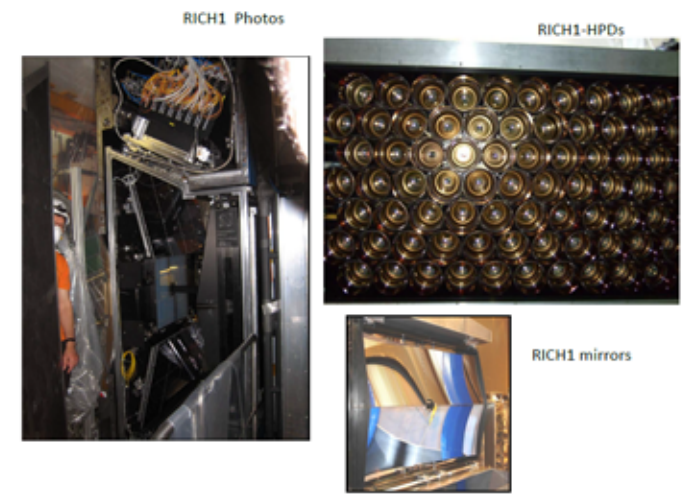
LHCb RICH

2014 F.Montanet Experimental Astroparticelle Physics ESIPAP



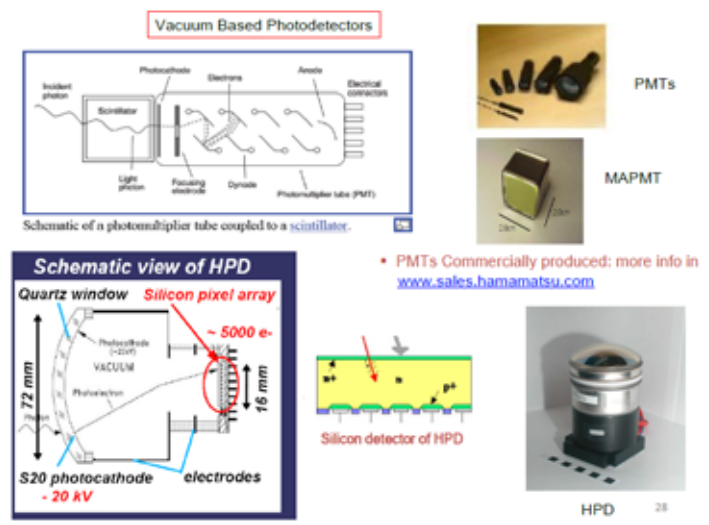
LHCb RICH

2014 F.Montanet Experimental Astroparticelle Physics ESIPAP



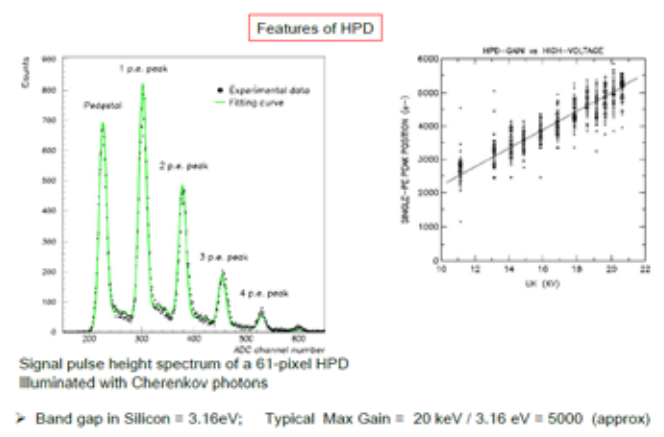
LHCb RICH

2014 F.Montanet Experimental Astroparticelle Physics ESIPAP



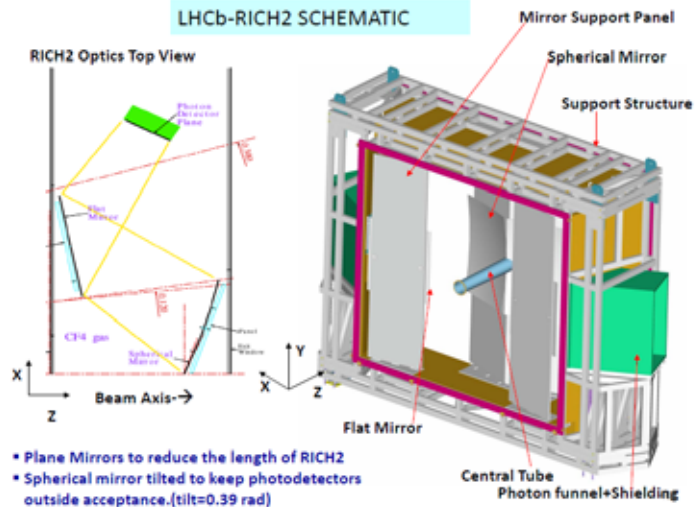
LHCb RICH

2014 F.Montanet Experimental Astroparticelle Physics ESIPAP



LHCb RICH

LHCb-RICH2 SCHEMATIC



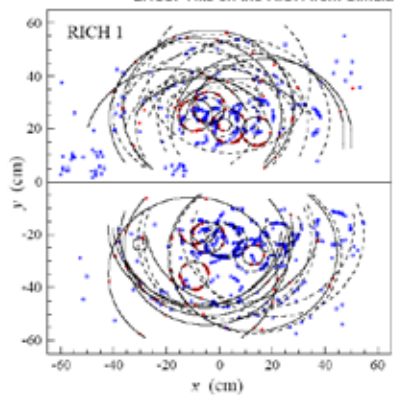
LHCb RICH

LHCb- RICH2 STRUCTURE



LHCb RICH

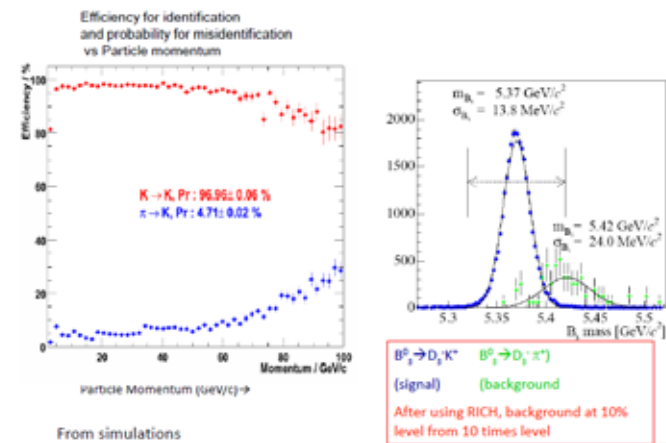
LHCb: Hits on the RICH from Simulation



Red: From particles from Primary and Secondary Vertex
Blue: From secondaries and background processes (sometimes with no reconstructed track)

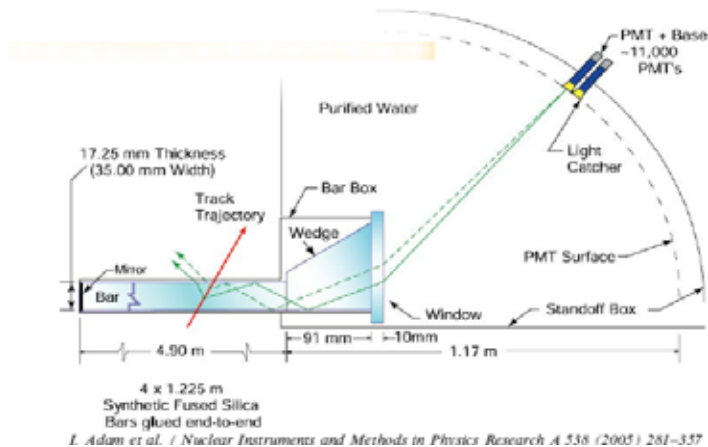
LHCb RICH

LHCb-RICH pattern recognition



A strange idea: the DIRC

- Detector of Internally Reflected Cherenkov light
- DIRC used at BaBar
- Turned out to be successful and robust for $\pi - K$ separation.



61

A strange idea: the DIRC

- Detector of Internally Reflected Cherenkov light
- DIRC used at BaBar
- Turned out to be successful and robust for $\pi - K$ separation.
 - Material is actually synthetic fused silica (Spectrosil)
 - Cross section 17.25 mm x 35.0 mm.
 - Four 1.225 m long bars glued together with Epotek 301-2 optical epoxy to make one 4.9 m long DIRC bar.
 - $99.9 \pm 0.1\%$ transmission per meter at 442 nm
 - $98.9 \pm 0.2\%$ transmission per meter at 325 nm



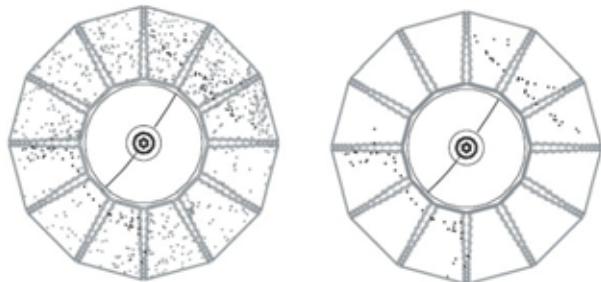
62

A strange idea: the DIRC

- Detector of Internally Reflected Cherenkov light

Reconstruction

- Arrival time is used to reduce background

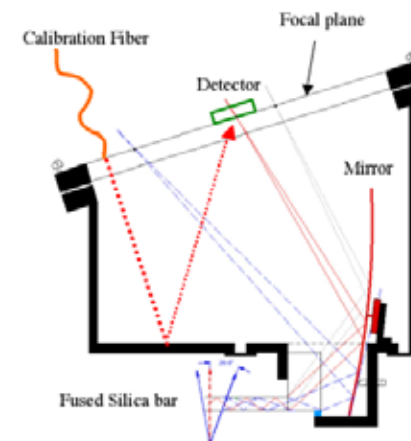


- Eliminating the photons outside of a ± 300 ns window around the trigger time yields a very clean signal

63

A strange idea: the DIRC

- Improving the DIRC concept: super-BELLE ?



64

IDENTIFYING PARTICLES

CHARGE MEASUREMENT OF PRIMARY CR

65

How to characterize the primary particle?

- Mass m
- Electric charge Ze
- Velocity $v = \beta c$
- Lorentz Facteur $\gamma = E/mc^2$
- Momentum $p = mc\beta\gamma$
- Kinetic energy $T = mc^2(\gamma - 1)$

66

How to characterize the primary particle?

Detector	Observable	Link with the particule
Magnetic spectrometer	Rigidity & Sign of Z	pc/Ze
Time of flight	Velocity/c	β
Proportionnal counters Scintillators Ionisation chamber	Ionisation	$dE/dx = Z^2 f(\beta)$
Čerenkov effect	Č photons density	$dN/dx = Z^2 g(\beta)$
Transition radiation	Number of photons X	$N = Z^2 h(\gamma)$
Calorimeter	Deposited energie	$mc^2(\gamma - 1)$

67

Two important radiations for particle identification

Two effects of the **polarization** induced by charged particles in dielectric medium

Proportionnal to Z^2

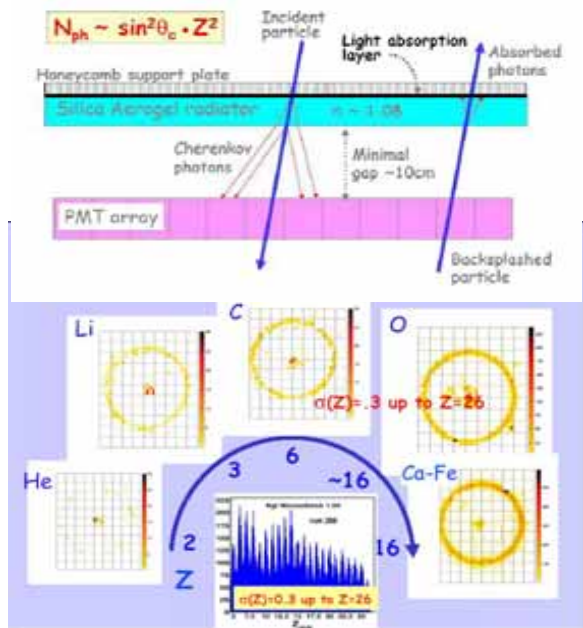
- **Čerenkov radiation** : si $v > c/n$
Sensitive to $\beta = v/c$
- **Transition radiation** : at the interface of \neq dielectric media
Sensitive to $\gamma = E/(mc^2)$

68

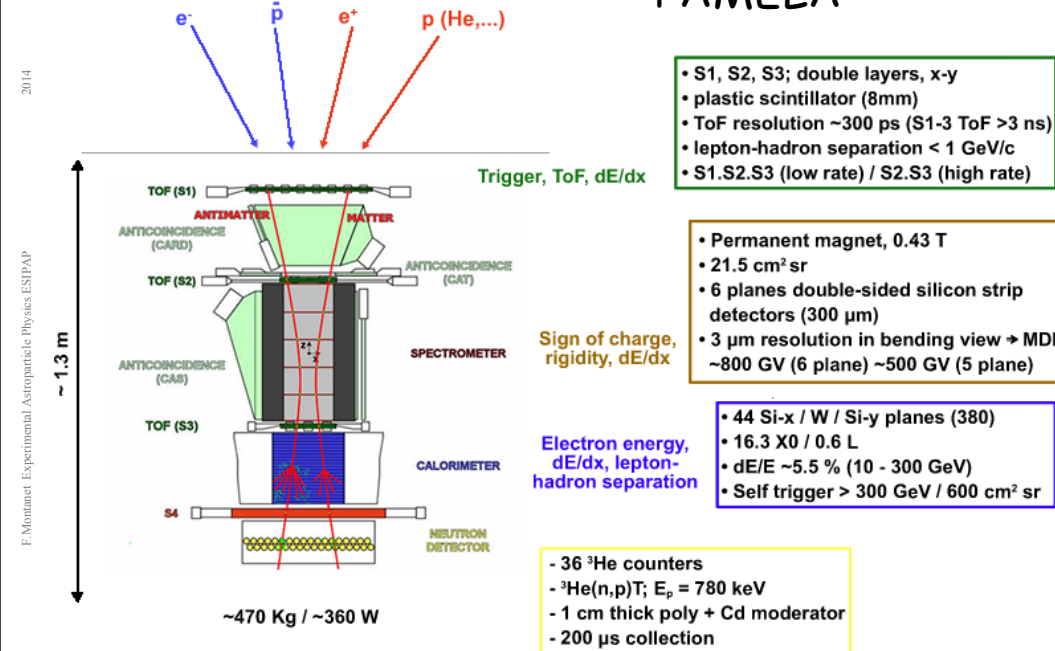
Cherenkov imaging (RICH) and charge measurement

RICH principle →

AMS 2 Prototype →



PAMELA



AMS-2 On Board ISS

Mission Number: STS-134
 Launch: May 19, 2011
 Orbiter: Endeavour



Space spectrometers

	AMS-1 (June 1998)	PAMELA (June 2006 - ...)	AMS-2 (May 2011 - ...)
Spectrometer Acceptance	0.82 m ² sr	20.5 cm ² sr	0.82 m ² sr
Spectrometer	Aimant permanent Nd Fe B 0.15 T BL ² = 0,15 T m ² 6 plans (Si)	Aimant permanent Nd Fe B 0.48 T BL ² = 0,10 T m ² 6 plans (Si)	Aimant permanent Nd Fe B 0.15 T BL ² = 0,15 T m ² 6 plans (Si)
Time of Flight	yes	yes	yes
Cherenkov	Aerogel (threshold)	-	Ring Imaging Ch.
Transition rad	-	yes	yes
Neutrons det.	-	³ He	-
Anticoincidence	-	yes	yes
Calorimeter	-	16,3 X ₀ W+22 plans (Si)	16 X ₀ Pb+fibers sc.

A precision, multipurpose spectrometer up to TeV

TRD
Identify e^+ , e^-

TOF
 Z, E



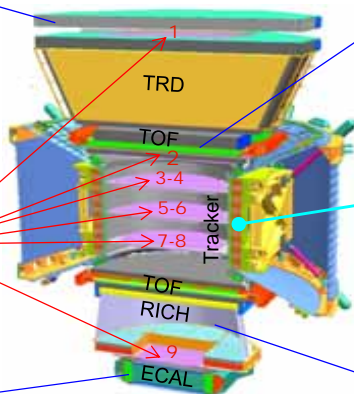
Silicon Tracker
 Z, P



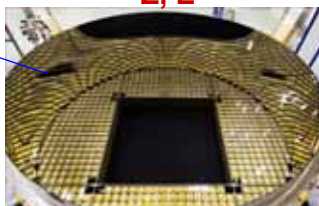
Magnet
 $\pm Z$



ECAL
 E of e^+ , e^- , γ



RICH
 Z, E

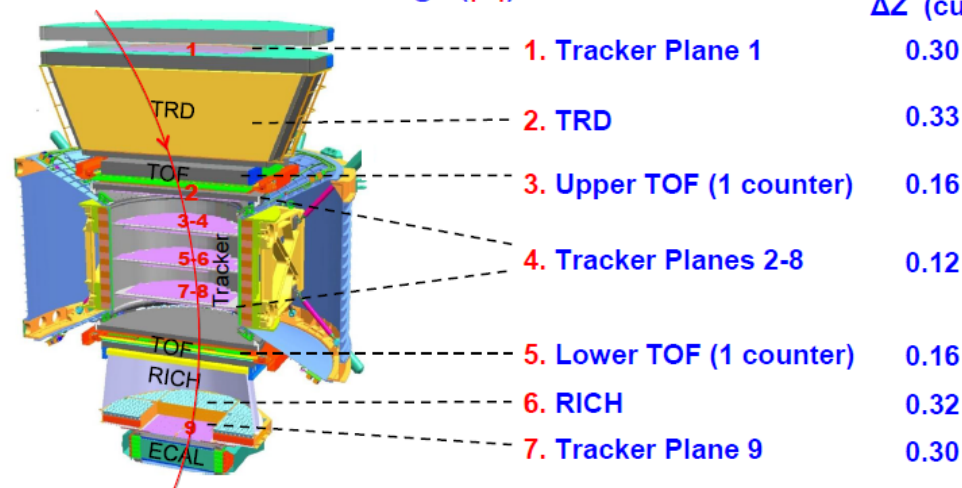


Z, P are measured independently by the Tracker, RICH, TOF and ECAL

AMS charge identification

AMS: Multiple Independent Measurements of the Charge ($|Z|$)

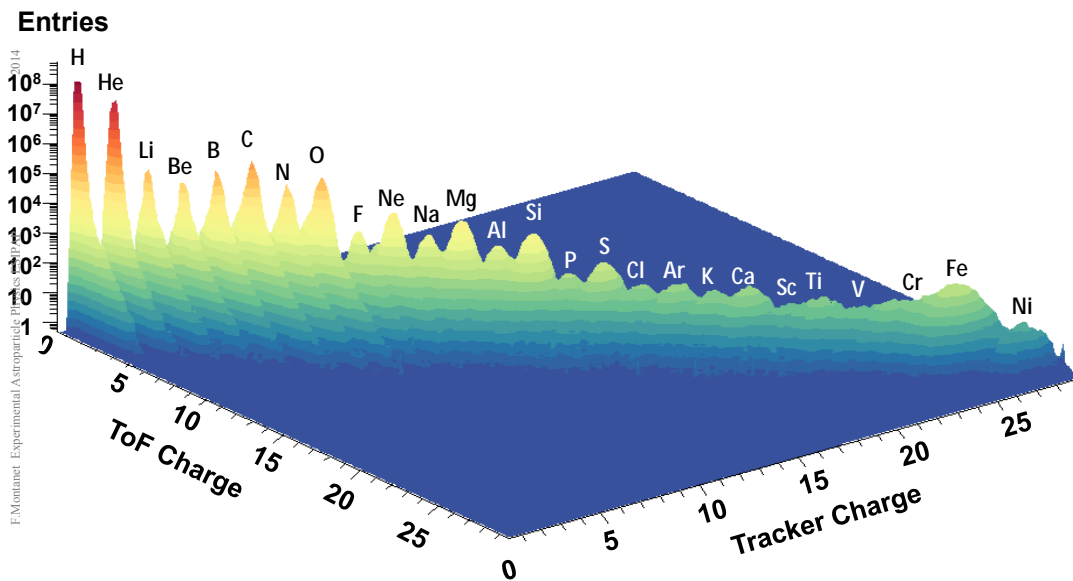
Carbon ($Z=6$)
 ΔZ (cu)



Full coverage of anti-matter & CR physics

	e^-	P	He, Li, Be, ... Fe	γ	e^+	\bar{P}, \bar{D}	\bar{He}, \bar{C}
TRD							
TOF							
Tracker							
RICH							
ECAL							
Physics example	Cosmic Ray Physics				Dark matter		Antimatter

AMS Nuclei Measurement on ISS





CREAM

Ultra Long Duration Balloon

ULDB Proj., Adv.Sp.Res33,1633(2004) :

NASA project to develop

- Flight of < 100 days
- Payload \leq 2 tons
- Alt 33000 meter
- CREAM n° 1 : 2006 (2005/LDB)

Experimental Astroparticle Physics ESIPAP

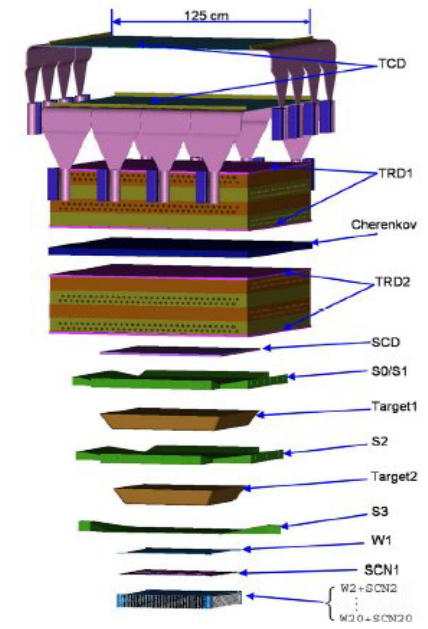


2014 F.Montanet Experimental Astroparticle Physics ESIPAP

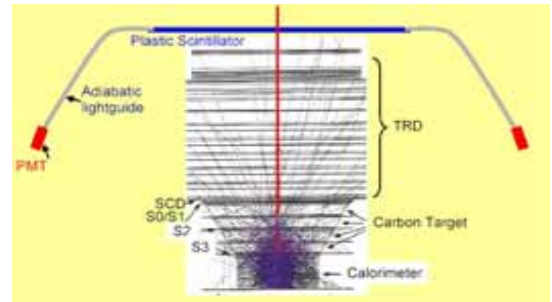
CREAM

Cosmic Ray Energetics and Mass

- **Objectives :**
CR composition and spectrum of the different elements (from TeV to ~500 TeV)
- **Acceptance :** 2,2 m² sr
- **Energy measurement:**
 - Calorimeter 20 X₀ (W + scint. fibres)
 - Transition Radiation Detector
- **Identification :**
 - TRD
 - Cherenkov detector "CHERCAM" similar to AMS-2



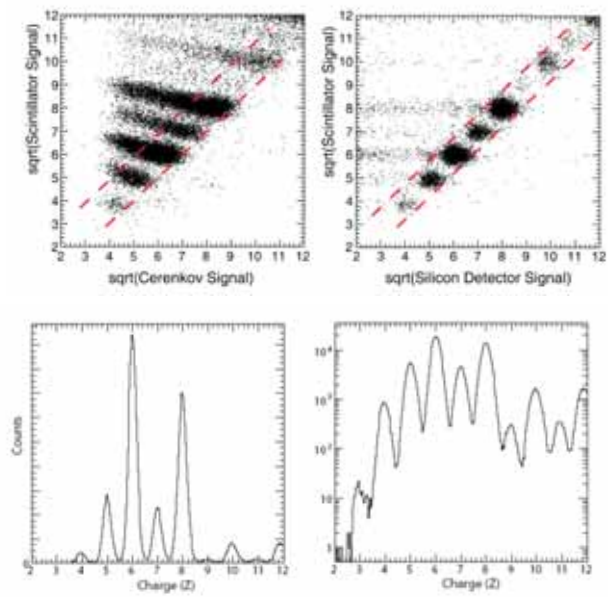
CREAM experiment



- **At TeV energies**, the interaction of CR in the calorimeter induces **many backscattered secondary particles** that one have to veto.
- The **"CHERCAM" cherenkov** solves this problem by measuring accurately the time of any through going particle as well as achieving a precise charge measurement ($\pm 0,3 e$)

2014 F.Montanet Experimental Astroparticle Physics ESIPAP

CREAM experiment

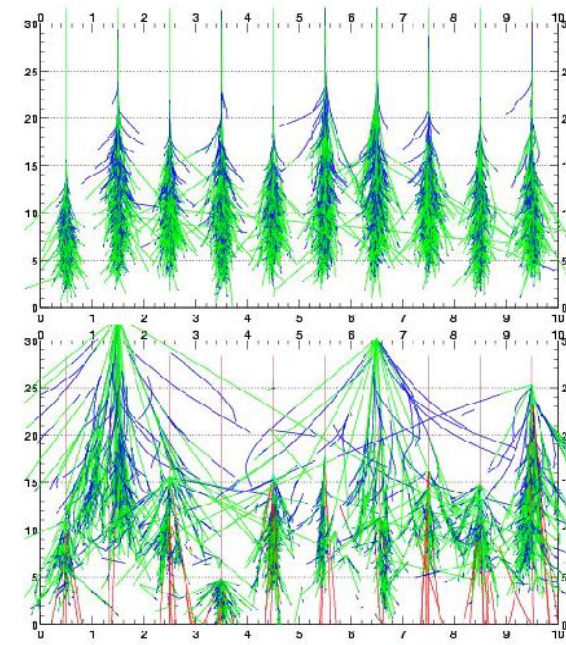


2014 F.Montanet Experimental Astroparticle Physics ESIPAP

ATMOSPHERIC GAMMA-RAY SHOWERS BY CHERENKOV TELESCOPES

10 γ
300 GeV

10 protons
300 GeV



Simulations de M. de Naurois

Electromagnetic showers (e^\pm or γ primary)

Dominating phenomena

- Radiation processes:
 - Bremsstrahlung of e^\pm
 - Pair production ($>MeV$) pairs e^+e^-
- Multiple scattering (small angular deflexions) of e^\pm
- Energy losses by e^\pm
 - par ionisation
 - excitation des atomes

In the coulombian field of nuclei

γ induced shower 300 GeV

Roughly symmetric around the axis

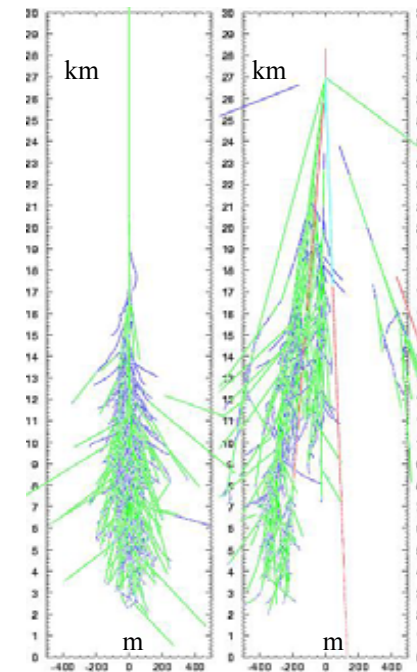
Small transverse dispersion (multiple scattering)

(almost) no muons

...

(unless $E_0 > 1$ PeV)

Essentially $e^+ e^-$ and γ secondaries



proton induced shower 300 GeV

Large transverse momentum

Muon component (from mesons decays)

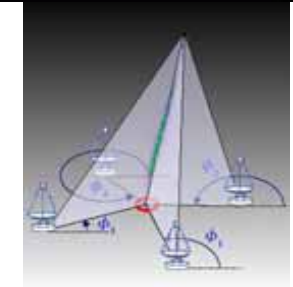
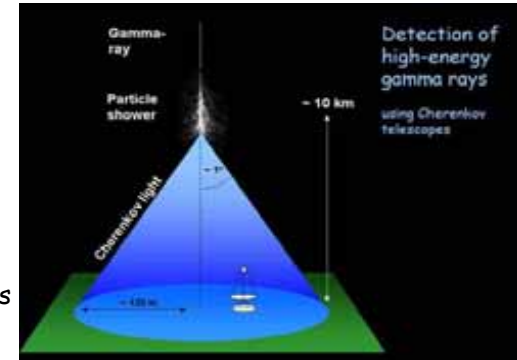
A hadronic shower does contain EM sub-showers

Optical photon emission by showers

- Showers charged particles emit light:
 - **Cherenkov light** : very collimated along the shower axis (Cherenkov angle at 1 Atm. $\approx 1^\circ$) threshold depending on the altitude : at ground 22 MeV for e^\pm et 4.5 GeV for μ^\pm
(20 photons per m per $\beta \approx 1$ charged particle at 1 atm)
Essentially used for gamma-ray astronomy
 - **Nitrogen fluorescence**: isotropic emission
(≈ 4 photons per electron per m)
Essentially used at UHE $\geq 10^{18}$ eV.
- This light detected by ground telescopes gives us very rich information on the **3D development of the showers**. It give a quasi calorimetric reliable measurement of the energy.
- ... but optical detectors can only work during moonless clear sky nights ($\approx 10\%$ duty cycle).

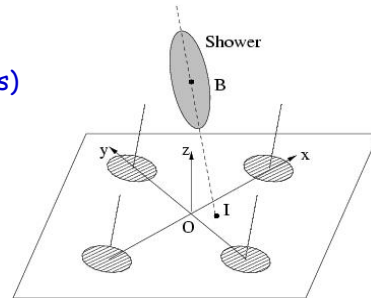
Cherenkov light from VHE gamma rays showers

- Shower front \approx conical at energies $>$ TeV, very well defined in time (few nanoseconds) ...
- ... ground enlightened area of 150 m radius at 1800m asl for TeV showers.
- Any large acceptance telescope in this area receive enough photons \rightarrow effective detection area $\sim 10^5$ m²
- With an array of such telescopes, **3D reconstruction of showers (stereoscopy)** \rightarrow total number of Cherenkov photons as an energy estimator).



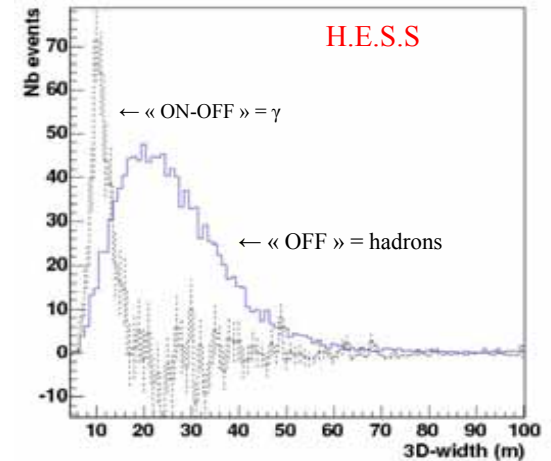
Showers Cherenkov light

- **Longitudinal profile**: similar to the particle density profile with a slight shift towards ground of $0.3 X_0$ due to the variation of the Cherenkov threshold with altitude.
- **Transverse profile**: much narrower than that of charged particles ($\sigma_T \approx 10$ to 15 m at 10 km altitude), threshold effect + energy of particles decreasing further away from axis.
- **The Cherenkov « photosphere »** (origin of photons distribution of EM showers) can be approximated by a 3D gaussian distribution, with axial symmetry for EM showers.
- **The measurement of the transverse standard deviation σ_T** allows distinguishing narrow EM showers from much wider hadronic showers, (transverse momentum of nuclear interactions \gg QED radiative processes).



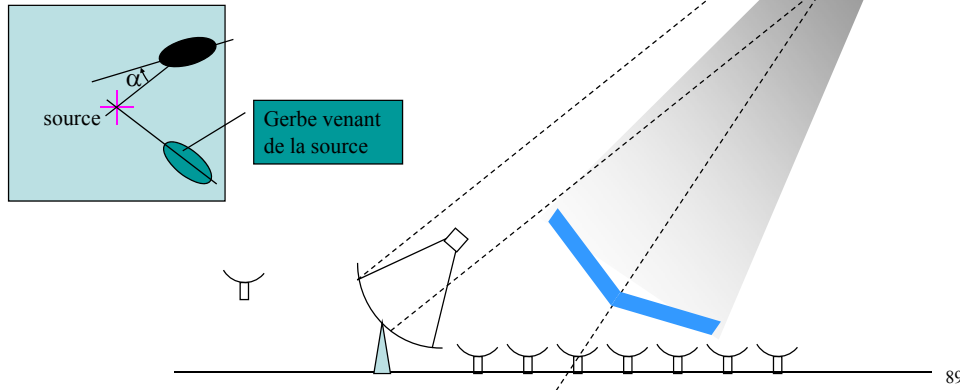
Cherenkov transverse profiles: EM versus hadronic showers

- « OFF » data: showers detected by 3 or 4 telescopes in a zone without γ sources $\rightarrow \sigma_T$ distribution for hadronic showers
- « ON » data : showers detected by 3 or 4 telescopes in the direction of the γ source PKS2155-304 (a blazar).
- « ON-OFF » distribution : $\rightarrow \sigma_T$ distribution for γ showers as seen by 3 or 4 telescopes.



VHE gamma-ray observation

- ACT, detection principle:
 - Imagers : WHIPPLE, CANGAROO, HEGRA, CAT
Hess, Magic, Veritas
 - Samplers : ASGAT, THEMISTOCLE,
HEGRA-AIROBICC, CELESTE, SOLAR2

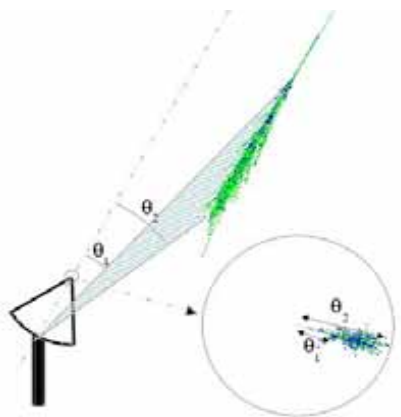


Gamma-ray astronomy above 100 GeV

- Atmospheric Cerenkov Detectors (ACTs)
 - Limited field of view instruments (5° de diamètre pour H.E.S.S.),
 \Rightarrow must follow the source apparent displacement on the sky.
 - Can follow only one source at the time.
 - Only work at clear sky moonless nights.
 - Great γ -hadron discriminating power \rightarrow most of the TeV sources discoveries.
- Surface detectors (charged particles and γ secondaries at ground level)
 - Large field of view (\approx steradian) instrument
 - High duty cycle
 - Low γ - hadron discrimination power \rightarrow limited sensitivity.

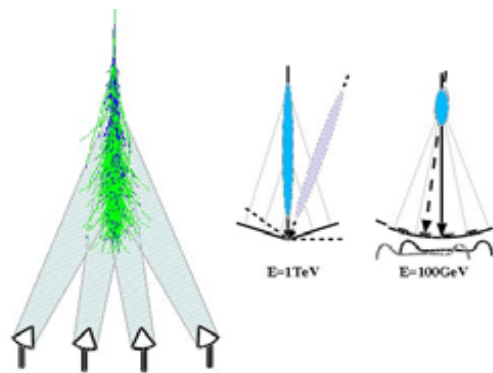
ACT

Imagers



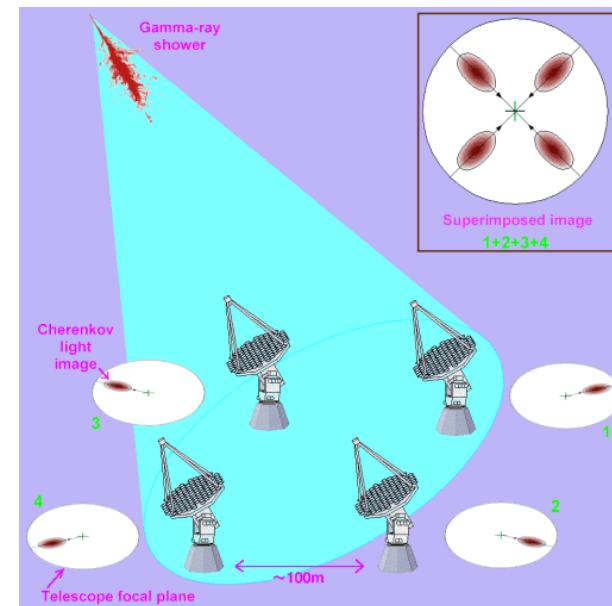
Form the shower image in the focal plane

Samplers



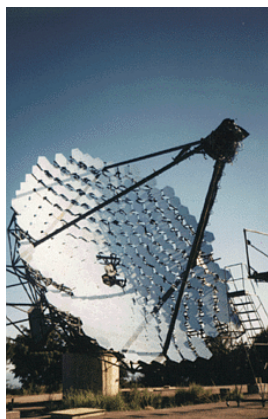
Arrival time + amplitudes on a large number of stations

ACTs in stereoscopic mode

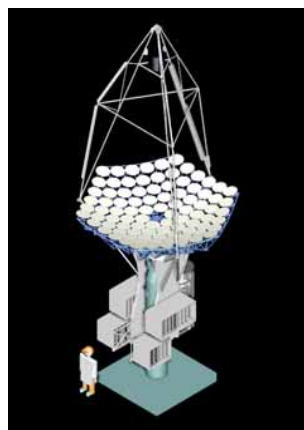


Former ACT

WHIPPLE



CAT



ACTs:

Lowering the energy threshold

Sky background $\sim 10^{12}$ photons $m^{-2} sr^{-1} s^{-1}$

$$\frac{\text{Signal}}{\sqrt{\text{sky bg}}} \propto \frac{A_{\text{col}} \tau \Omega_g \epsilon}{\sqrt{A_{\text{col}} \Delta t \Delta \Omega \epsilon}} \propto \sqrt{\frac{A_{\text{col}} \epsilon}{\Delta t \Delta \Omega}}$$

- Increase the photons collection area \approx reflector area A_{col}
- Increase the photon detection efficiency ϵ (mirror reflectivity, light funnels, PMTs quantum efficiency)
- The coincidence time gate Δt should not exceed by much the Cherenkov characteristic time ($\tau \approx 3$ ns) \rightarrow **isochrones mirror, fast triggering**
- The solid angle $\Delta \Omega$ within which the photon signal is integrated should not exceed much the angular size of the shower Ω_g
 \rightarrow **small pixels, triggering by fraction of the field of view or using nearby pixel patterns.**

Current ACTs

Observatory	# of telescopes	Reflector diameter (m)	Site
CANGAROO III	4	10	Australia
HESS I	4 \rightarrow 4+1	12 (28)	Namibia
MAGIC	1 \rightarrow 2	17	Canaries
VERITAS	2 \rightarrow 4	12	Arizona

VERITAS



CANGAROO III



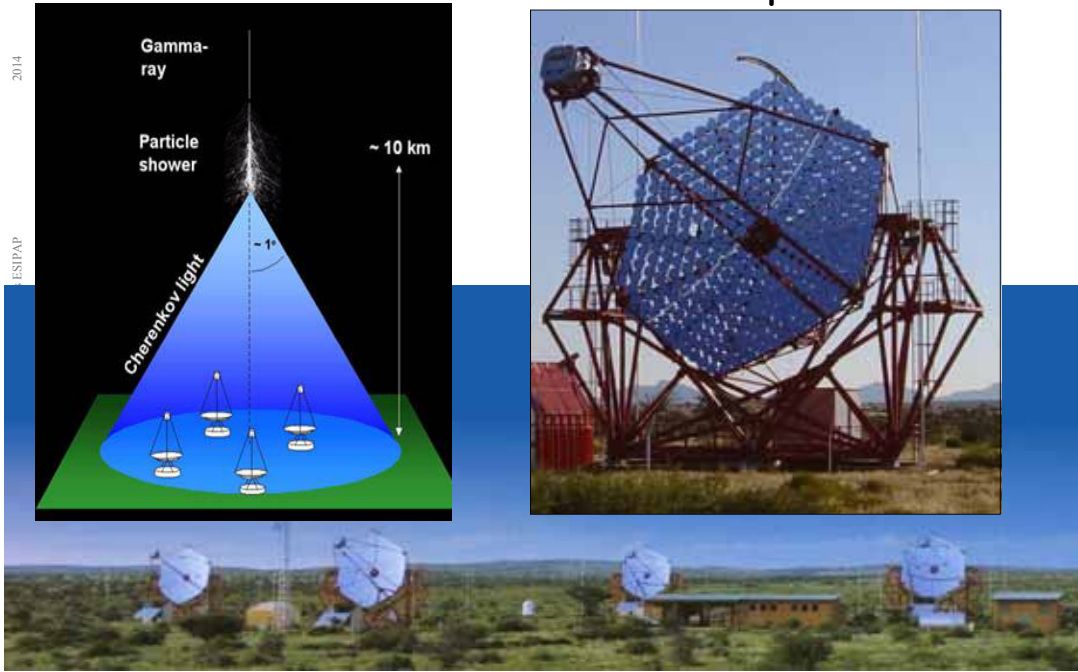
MAGIC



HESS I



Hess 2004 : x4 telescopes



Imaging telescopes: the cameras

Experiment	# pixels	Pixels size	Field of view
CANGAROO III	552	0.115°	3°
HESS I	960	0.16°	5°
MAGIC	396+180	0.08°-0.12°	4°
VERITAS	499	0.15°	3.5°

2014
F.Montanet - Experimental Astroparticle Physics ESIPAP

98

Imaging telescopes: high resolution cameras



VERITAS



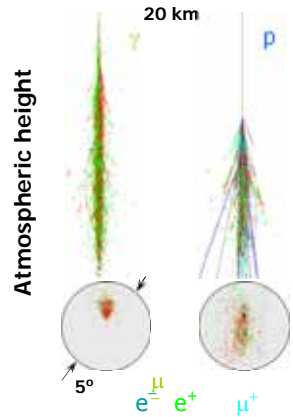
MAGIC

Imaging telescopes: high resolution cameras (H.E.S.S.)

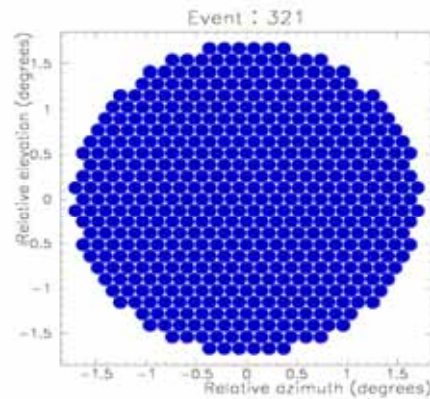
- 960 phototubes equipped with light funnels (Winston cones).
 - On board trigger electronics (partially overlapping sectors)
 - On board continuous analog memory and fast (Ghz) sampling (Analog Ring Sampler) + integrated signal 12 ns → ADC
- 2014
ESIPAP
- F.Montanet - Experimental Astroparticle Physics ESIPAP



99

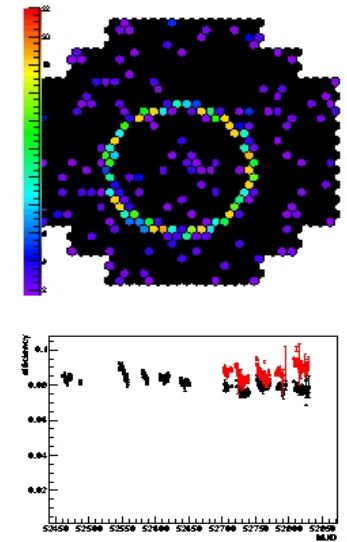


VERITAS Movie Camera



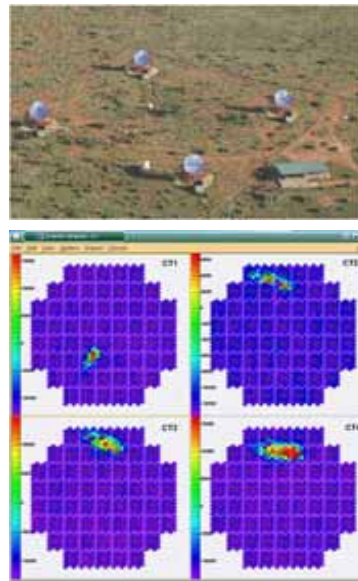
An effective detector monitoring: muon rings

- Muons through the mirror produce a perfect ring image whose light content is completely computable.
- Comparing measured signals with estimations \rightarrow global efficiency including effects such as :
 - near atmosphere absorption;
 - mirror reflectivity;
 - light collection;
 - PMTs quantum efficiency .
- The detector monitoring is then automatically taken into account in the data analysis.



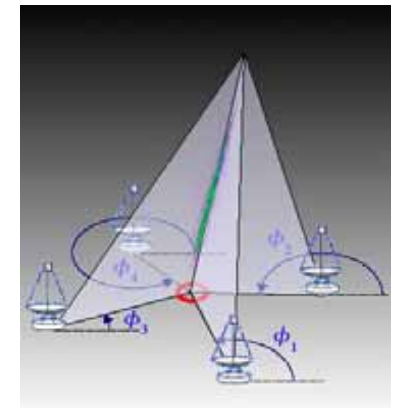
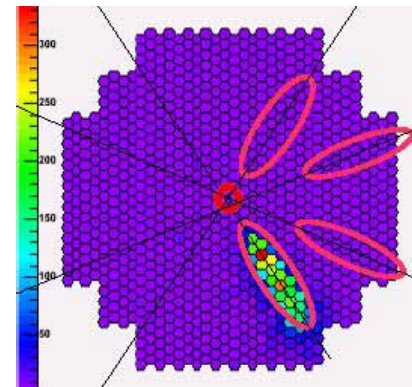
Stereoscopic ACTs

- Each showers is seen by many telescopes
- Very high hadron shower rejection factor (> 1000)
axial symmetry + narrow 3D width + punctual source pointing
- Much improved angular resolution wrt 1 telescope ($\approx 4'$ avec 4 télescopes)
- Better energy resolution ($\approx 15\%$)

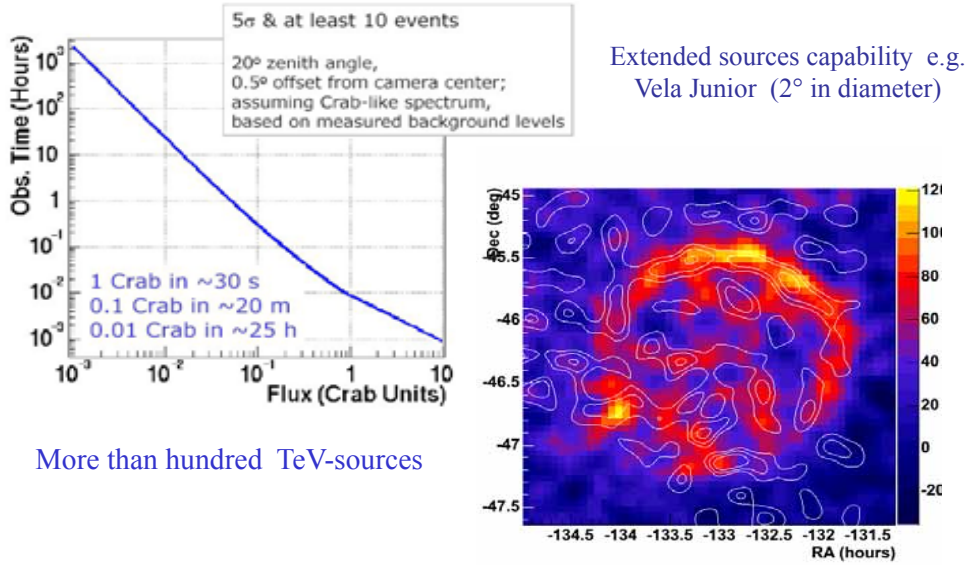


Stereoscopic ACTs

- Direct measurement of the origine of the gamma-ray in the field of view (important for extended sources)
- Direct measurement of the ground impact point (important for the determination of the energy)



Sensitivity to gamma-ray sources: H.E.S.S.

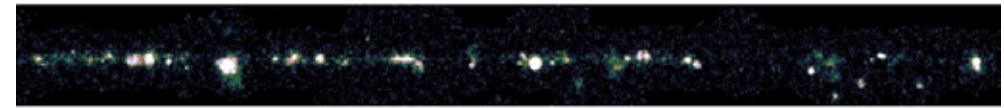


More than hundred TeV-sources

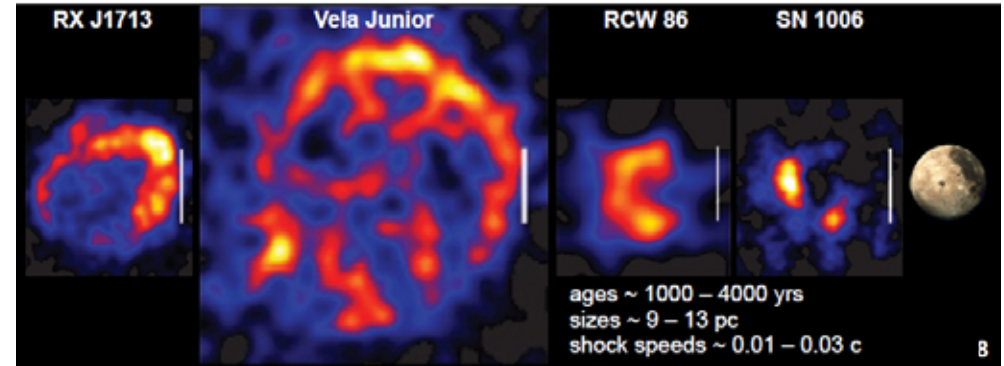
M. Lemoine-Goumard 2006

Galactic Plane Survey with H.E.S.S.

- ~2800 hr of observations of the inner Galaxy (2004–2012)
 - ~100 sources above the H.E.S.S.-I sensitivity ~1% of Crab
 - Large variety of source types & ~1/3 of unidentified sources

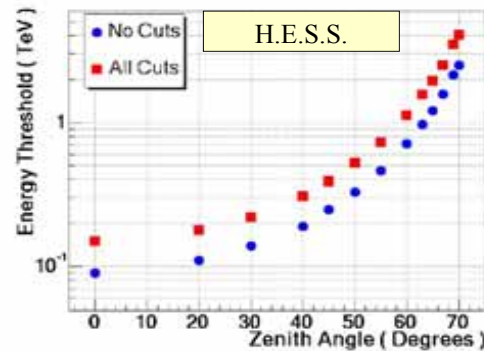


5 resolved shell-type SNRs

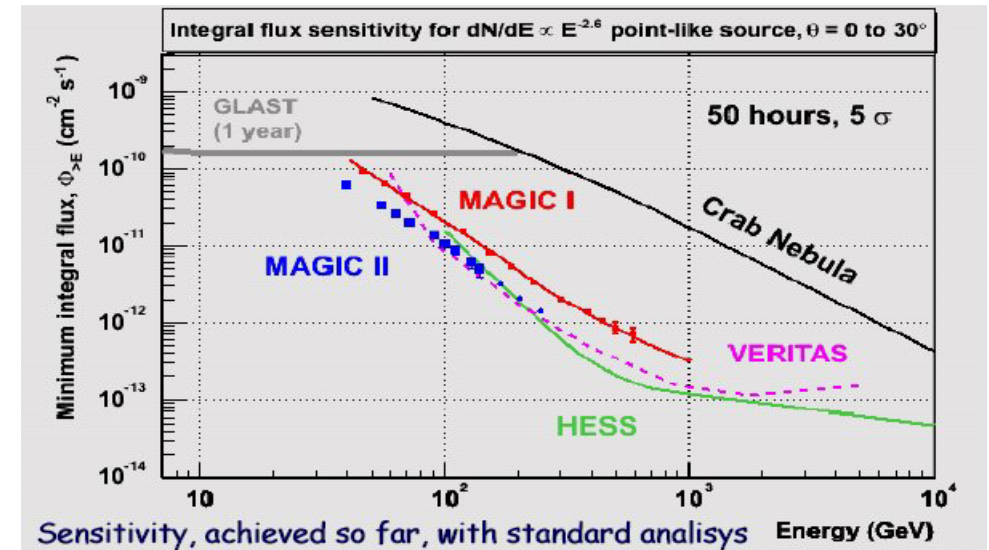


Energy threshold

- The threshold depends on the zenith angle
- Typically 120 GeV at the zenith for H.E.S.S. and comparable stereoscopic systems.
- **MAGIC II** (2 identical large telescopes) down to 50 GeV.
- **Starting now: H.E.S.S. II**
 - 50 GeV with a very large telescope + les 4xHESS I in stereo
 - 20 GeV expected in « mono » with HESS II large telescope and a second level trigger.



Sensibilités des télescopes d'imagerie actuels



Down to 20 et 50 GeV with H.E.S.S. II

2014 F. Montanet: Experimental Astroparticle Physics ESIPAP


HESS I (4x LCT)

Event Classes :

1. Mono : VLCT
2. Stereo : VLCT = LCT or LCT - LCT

Very Large Cherenkov Telescope

MAN Design: conventional all-az mount



Very Large Cherenkov Telescope:

- Reflector : 28 m \varnothing ($\approx 600 \text{ m}^2$)
- Focal distance $\approx 35 \text{ m}$
- Camera: 2.5 m \varnothing ($\approx 3 \text{ t}$)
- 2048 PMTs (0.07°/pixel)
- FoV : 3° \varnothing

- Trigger rate 2-20 kHz
- Faster analogue memories needed
- Optimize data flow: 2nd level trigger

HESS II

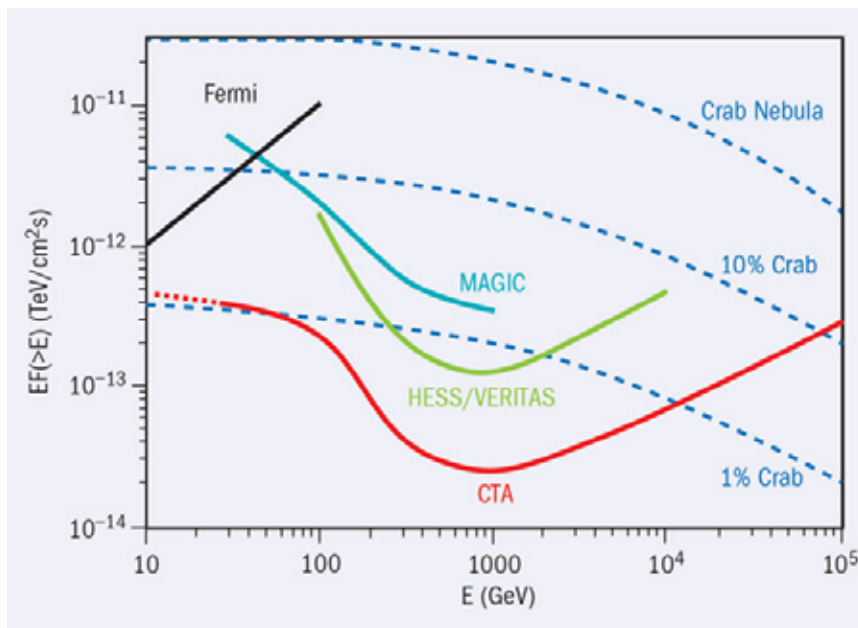
2014

- First light July 2012



The FERMI, MAGIC , H.E.S.S. II and CTA era

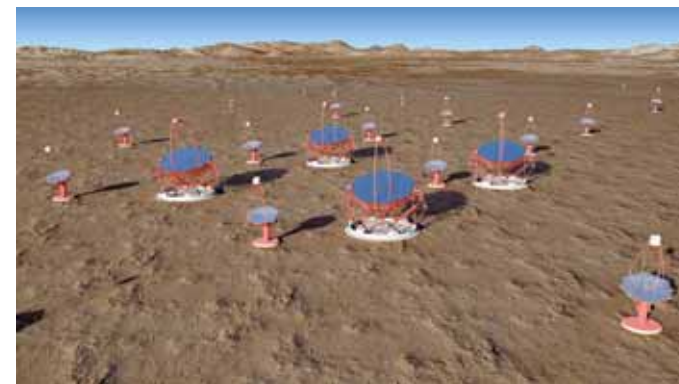
2014 F. Montanet: Experimental Astroparticle Physics ESIPAP



Toward a large array of ATCs : CTA

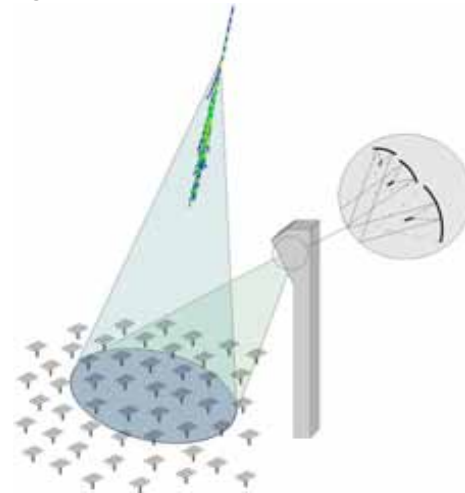
2014 F. Montanet: Experimental Astroparticle Physics ESIPAP

- Goal : a **milli-Crab** sensitivity at the **TeV**
- This could be achieved with 20 to 30 imaging telescopes (HESS-I type)
- The sensitivity is not only increased because of the **covered area**, but also due to improved **stereoscopic quality** (improved **hadron rejection factors** and **angular résolution**) : 56% of the showers seen by at least 4 tel with 16 in total, up to 2/3 with 36 tel.
- International consortium HESS-MAGIC-VERITAS, 2 sites one north one south: **CTA = Cherenkov Telescope Array**.



A (once favoured) alternative solution: sampling arrays

- To lower threshold, benefit of the very large mirror area from solar power plants
~ 2000 - 6000 m²
- Need to split the beam from the different heliostats
→ Secondary optics
- One PMT per heliostat.



CELESTE (France)

53 × 54 m²

STACEE (USA)

64 × 40 m²



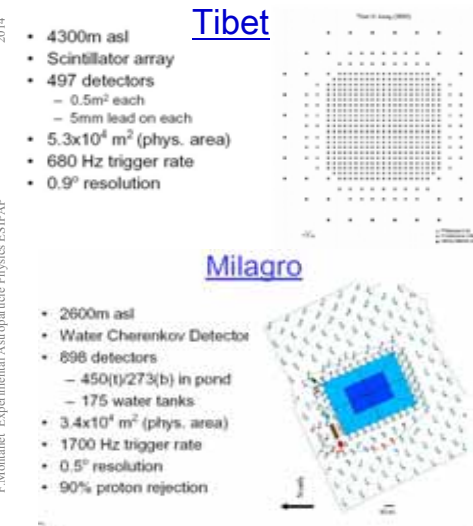
CACTUS (USA)

160 × 40 m²

Large field of view gamma-ray detectors

- Detect the shower particle reaching ground (at high altitude) (scintillateurs, RPCs or water Cherenkov detectors)
- Large duty cycle ≈ 90%
- Large solid angle ~ steradian
- Well suited to look for unpredictable transient phenomena (ex: gamma-ray burst)
- ... BUT small sensitivity (~0.5 Crabe) because of rather poor hadron shower rejection factor and limited angular resolution (0.5° to 1°); (measured from timing in different detectors).
- ... as well as rather high threshold (~ 1 TeV)

Large field of view gamma-ray shower detectors



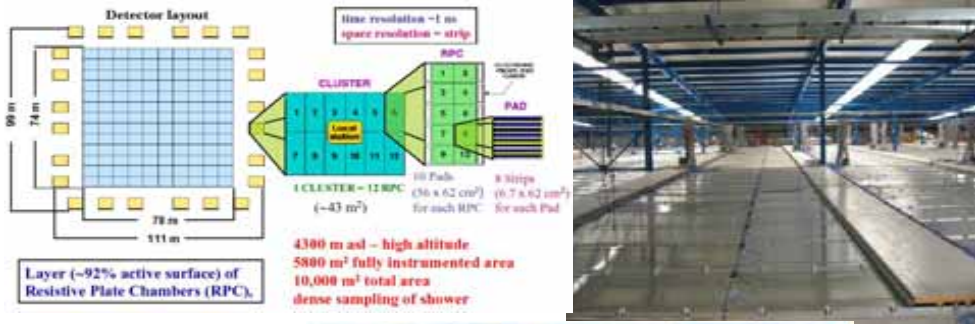
Scintillators



« water pool »

(water cherenkov detectors)

ARGO-Yang Ba Jing (2006)



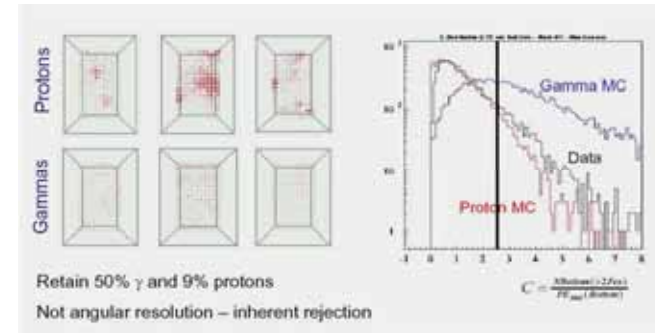
sensitivity ($\times 3$)



117

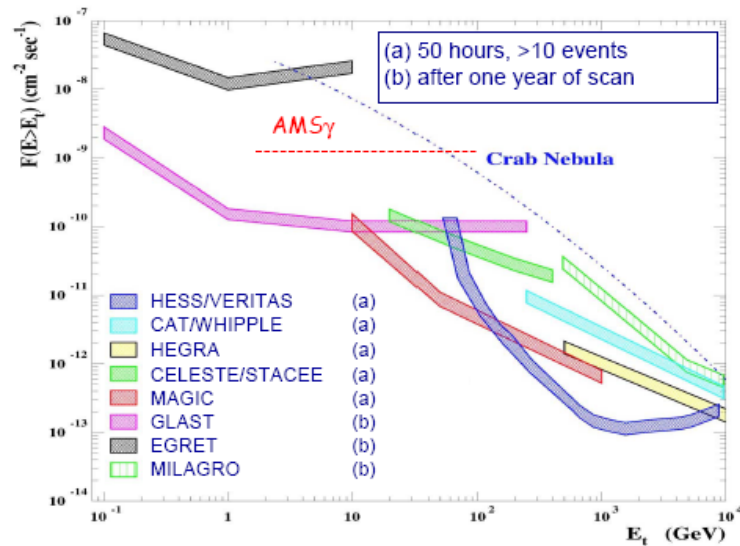
Hadronic background rejection by MILAGRO

- Cherenkov light in the deeper PMTs \rightarrow hadrons (cf. muons that traverses completely the pool).
- **Hadronic showers**: irregular light distribution \rightarrow less PMTs hit but larger signal each
- **EM showers**: more regular light distribution \rightarrow many more PMTs hit with small signal each PMT.



118

Nouvelle et futur génération de détecteurs gamma au sol



119

NEUTRINO TELESCOPES

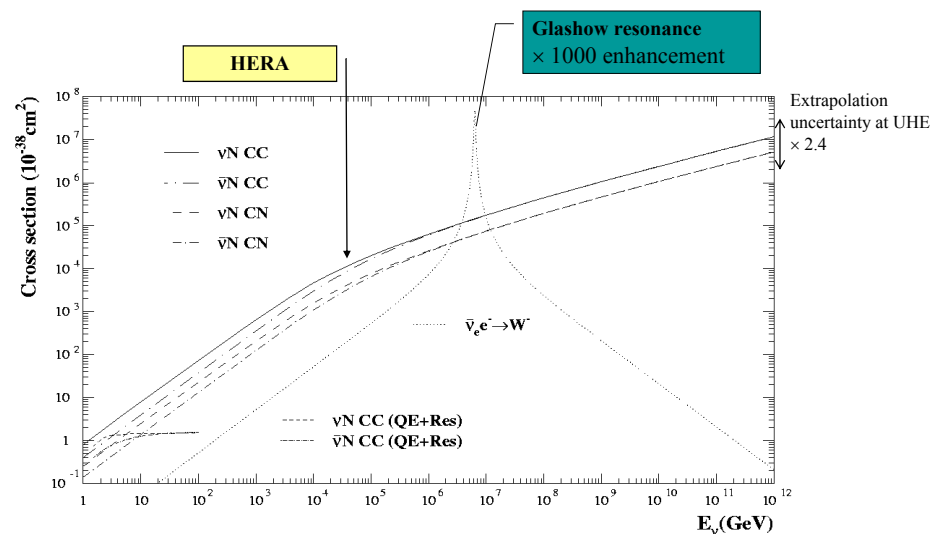
120

The cosmic neutrino spectrum, from MeV to EeV

- **MeV-GeV:** Solar neutrinos solaires & super Novæ, atmospheric neutrinos: various detectors but mostly a water cherenkov domain with **SuperKamiokande**
- **GeV-TeV:** Cherenkov in natural water or ice, neutrinos atmospheric neutrinos and beyond. **ICECUBE, ANTARES.**
- **TeV-PeV:** the same but extended to 1 km³ size. **ICECUBE** so far the only one.
- **EeV:** arrays foreseen for UHECR detection proved to be very efficient for UHEν's. Observe quasi horizontal or upgoing showers. **AUGER.**

Neutrino cross sections

- ν-matter cross sections:



Neutrino detectors

... super heavy weight category !



ex. the WBB of CERN :

$$10^{13} \text{ 400 GeV protons per extraction}$$

$$\Rightarrow \phi_\nu \approx 10^6 \text{ v cm}^{-2} \quad \langle E_\nu \rangle \approx 20 \text{ GeV}$$

avec :

$$\sigma_{\nu, N} = 0.6 \times 10^{-38} \text{ (E/GeV)} \text{ cm}^2 \text{ GeV}^{-1}$$

$$N_A = 6.02 \times 10^{23} \text{ mol}^{-1}$$

With a 100 tons detector, one gets:

$$\begin{aligned} N_{\text{evt}} &= N_{\text{nucl}} \times \phi_\nu \times \sigma_{\nu, N} \\ &= 6.02 \times 10^{23} \times 10^8 \times 10^6 \times 0.6 \times 10^{-38} \times 20 \\ &= 7,2 \text{ events / extraction} \end{aligned}$$

$$\sigma(\nu N) \sim 0.6 \times 10^{-38} \times \left(\frac{E_\nu}{1 \text{ GeV}} \right) \text{ cm}^{-2}$$

GeV detection with SuperKamiokande

Atmospheric neutrino flux:

$$\phi \sim 2 \text{ cm}^{-2} \text{ s}^{-1} \text{ sr}^{-1}$$

$$\lambda = \frac{1}{\sigma n}$$

Interaction probability: $P(x) = 1 - \exp\left(-\frac{x}{\lambda}\right) = 1 - \exp(-n\sigma x)$

$$n = \rho N_A$$

Interaction length λ: $\lambda \sim (6 \times 10^{23} \times 10^{-38})^{-1} \sim 1.7 \times 10^{14} \text{ cm}$

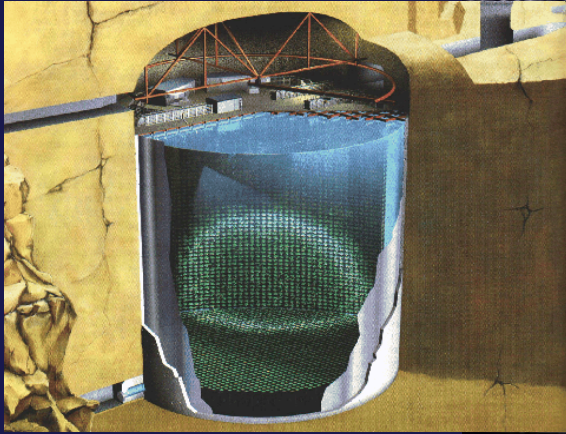
thus : $P(L) \sim \left(\frac{L}{1m} \right) \times 6 \times 10^{-13}$

Number of events per day in a detector of volume V=SxL

$$\begin{aligned} N &= \phi \Omega S P(L) \\ &\approx (2 \cdot 10^4 \text{ m}^{-2} \text{ sr}^{-1} \text{ s}^{-1}) \times (4\pi \text{ sr}) \times (8 \cdot 10^4 \text{ s}) \times 6 \cdot 10^{-13} \times V \\ &\approx 1.2 \times 10^{-2} \text{ events/day / m}^3 \text{ of water} \end{aligned}$$

Super Kamiokande

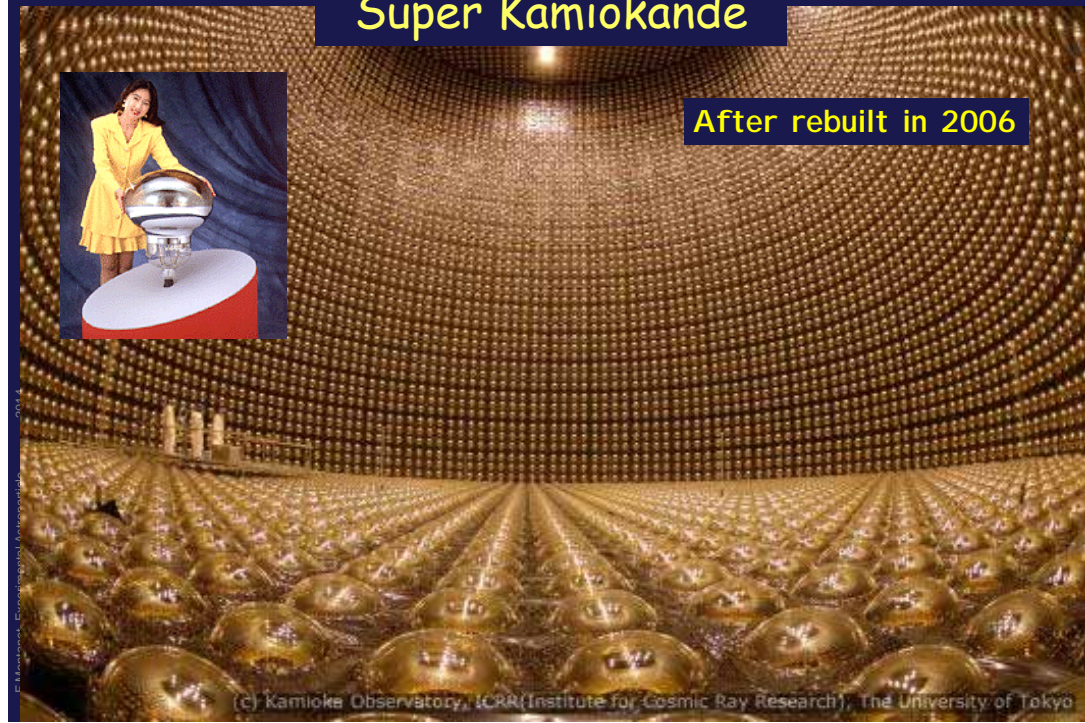
- Super-Kamiokande, détecteur souterrain au Japon, 50000 tonnes d'eau, 12000 PM de $\varnothing=50\text{cm}$.



- Water Cherenkov type Detector
- 22.5 kton Fid. Volume
- Concentric Cylindrical Shape
- 11146 PMTs for Inner Detector
- 1885 PMTs for Outer Detector
- Run from Apr. 1996 to Jul. 2001

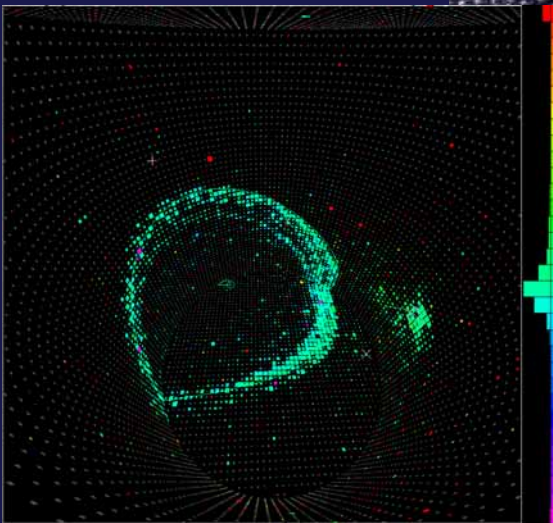
Super Kamiokande

After rebuilt in 2006

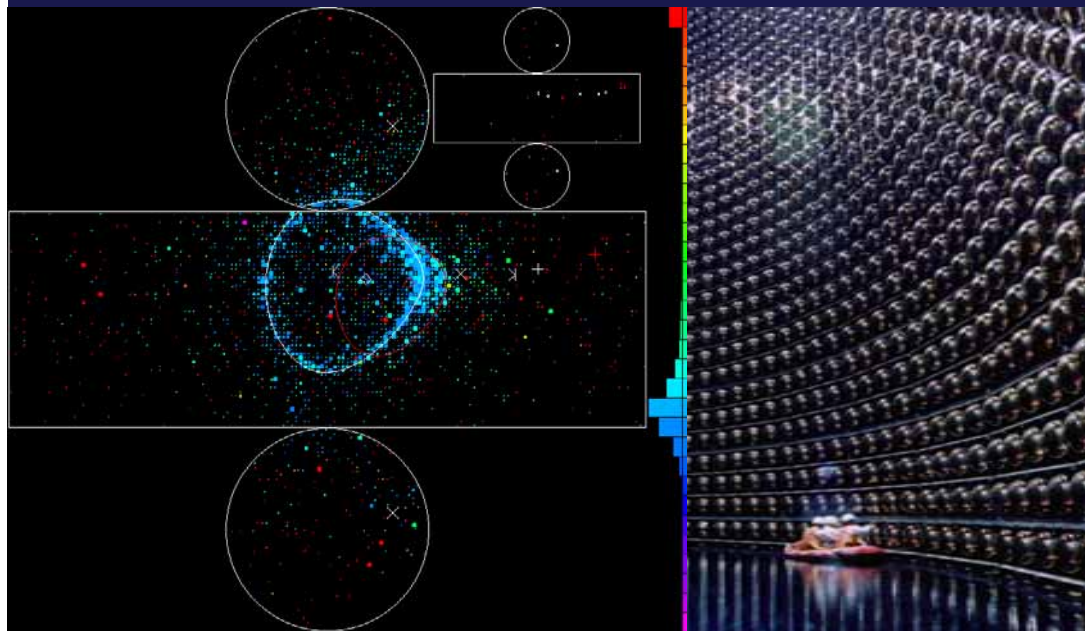


(c) Kamioka Observatory, ICRR (Institute for Cosmic Ray Research), The University of Tokyo

Super Kamiokande



Super Kamiokande



Event patterns in Super-Kamiokande

Fully Contained (FC) event

- All visible particles are contained in the detector both ν_μ, ν_e via NC or CC interaction
- Typically $E_\nu = 1 \text{ GeV}$
- Particle ID

Partially Contained (PC) event

- At least 1 charged particle escapes from detector
- ν_μ CC (97%)
- Typically $E_\nu = 10 \text{ GeV}$

Upward-going muons (Up-mu)

- Entering muon from below
- ν_μ CC only
- $E_\nu = 10 \text{ GeV}$ (stopping), 100 GeV (through-going)

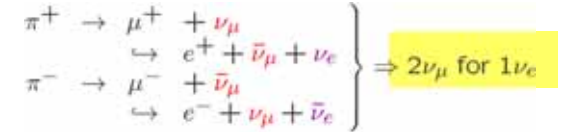
Super-Kamiokande covers $E_\nu = 100 \text{ MeV} \sim \text{over } 1 \text{ TeV}$

MZR PSA - 2008-2009
François Montanet LPSC/UJF

Atmospheric neutrinos

- Atmosphere :
 - $\sim 1000 \text{ g/cm}^2$
 - $\sim 20 \text{ km}$
 - 11 nuclear λ_{int}

- ν dominated by :



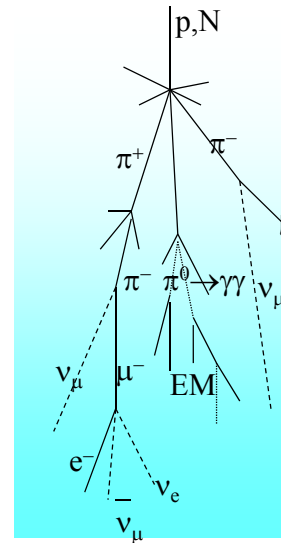
- Kinematics :

$$\begin{aligned} \pi^+ &\rightarrow \mu^+ + \nu_\mu & \mu^+ &\rightarrow e^+ + \nu_e + \bar{\nu}_\mu \\ \langle E_\mu \rangle &= 0.787 E_\pi & \langle E_\nu \rangle &= 1/3 E_\mu \\ \langle E_\nu \rangle &= 0.213 E_\pi \end{aligned}$$

$$\Rightarrow \langle E_{\nu_\mu} \rangle : \langle E_{\nu_e} \rangle : \langle E_{\bar{\nu}_\mu} \rangle \approx 1 : 1 : 1$$

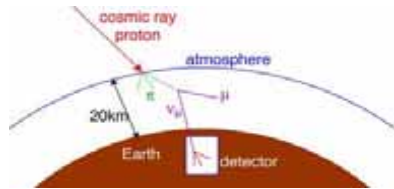
- 1 GeV sea level neutrino flux:

$$\phi \approx 2 \text{ cm}^{-2} \text{ s}^{-1} \text{ sr}^{-1}$$



MZR PSA - 2008-2009
François Montanet LPSC/UJF

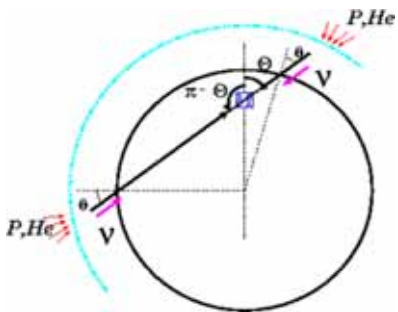
Atmospheric neutrinos



- Flavor ratio

$$\frac{\nu_\mu + \bar{\nu}_\mu}{\nu_e + \bar{\nu}_e} \approx 2 \text{ for } E_\nu \leq \text{qq GeV}$$

$$> 2 \text{ for } E_\nu > \text{qq GeV}$$



- top down symmetry for $E_\nu > \text{qq GeV}$

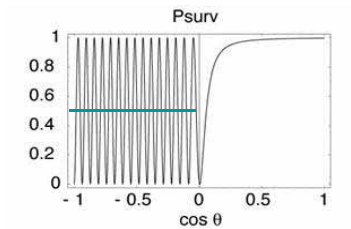
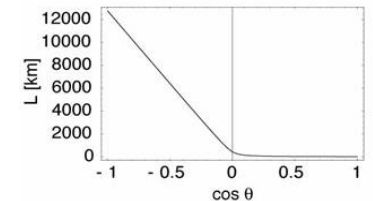
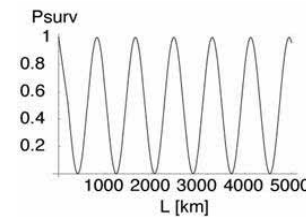
Distance traveled : $L_\nu = 10 \text{ to } 13000 \text{ km}$

MZR PSA - 2008-2009
François Montanet LPSC/UJF

Survival probability

$$p = 1 \text{ GeV}/c, \sin^2 2\theta = 1$$

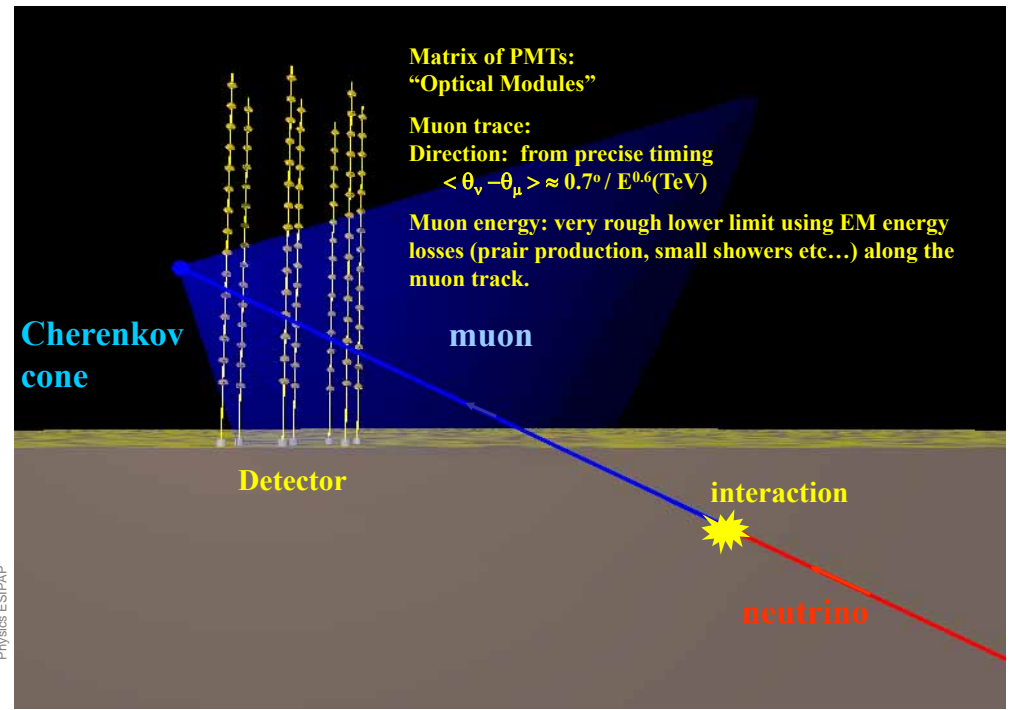
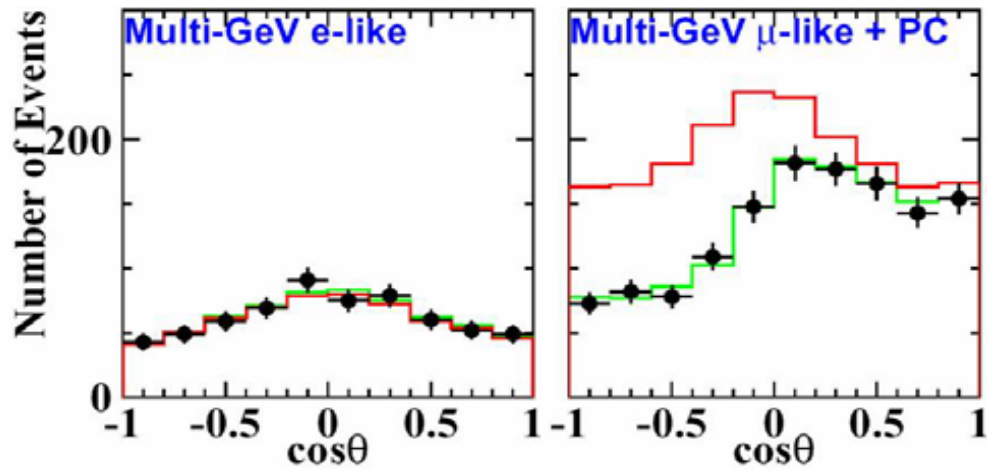
$$\Delta m^2 = 3 \times 10^{-3} \text{ (eV}/c^2)^2$$



Half of upgoing ν_μ are lost.

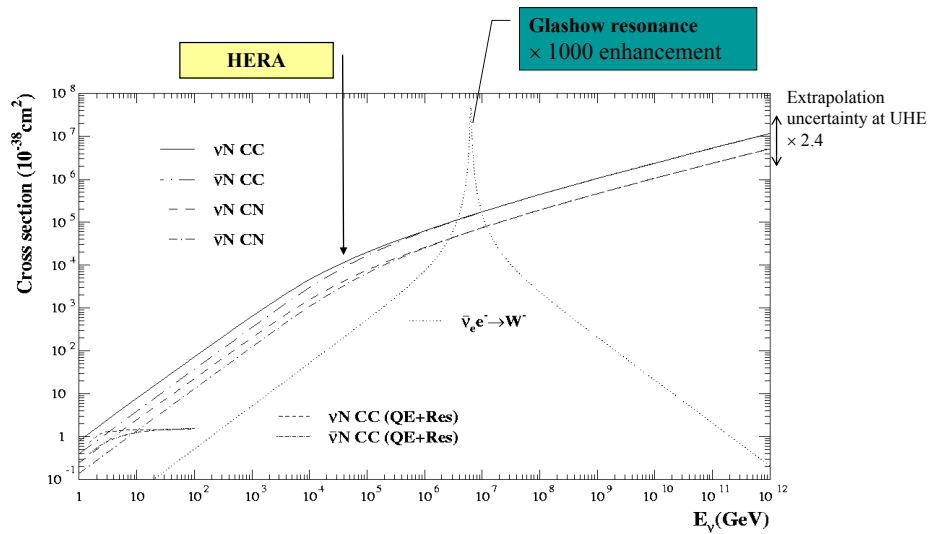
MZR PSA - 2008-2009
François Montanet LPSC/UJF

Half of ν_μ disappeared !

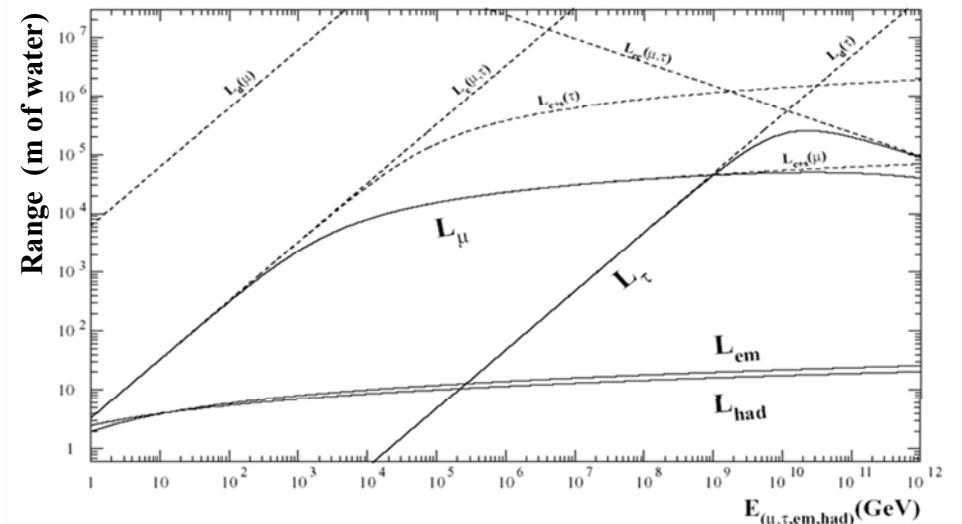


Neutrino cross sections

- v-matter cross sections:



Particle Ranges



Earth opacity

The earth is transparent to ν_μ < 100 TeV

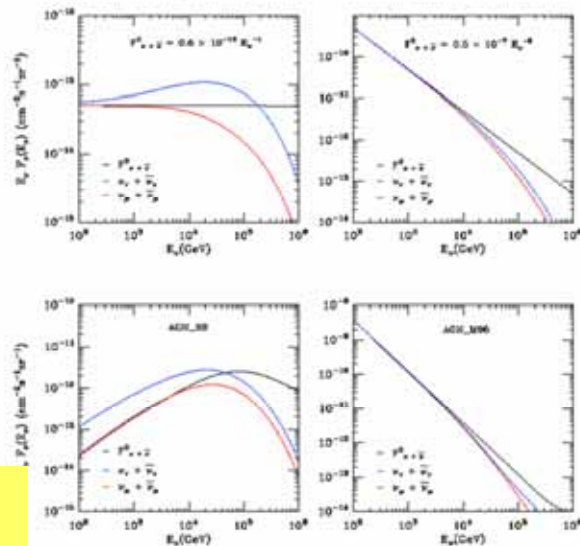
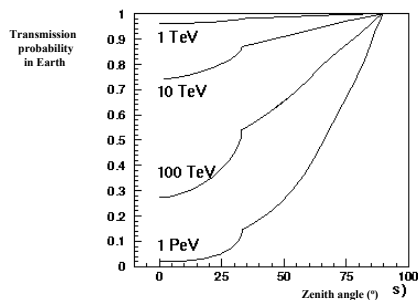
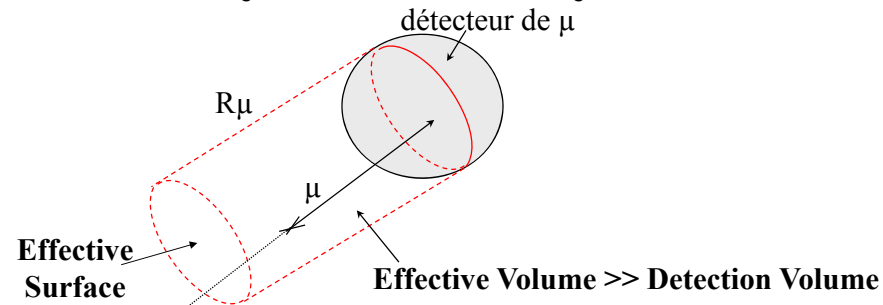


FIG. 2. Mean neutrino flux with direction flux (black lines), the effect of ice attenuation for $\theta = 0^\circ$ (red lines) and ice attenuation plus regeneration upward flux for the same zenith flux and the same zenith angle (blue lines for a) E^{-1} flux b) E^{-2} flux c) AGN_SS and d) AGN_MPS.

ν_μ absorbed via cc, or regenerated via nc
 ν_τ regenerated via cc because $\tau \rightarrow \nu_\tau$ before interacting or significant energy loss.

Detection principles

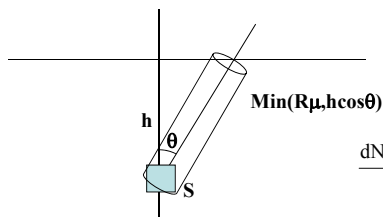
- The effective target volume is \propto the muon range



$$V_{\text{eff}}(E_\mu) = A_{\text{eff}}(E_\mu) \cdot R_\mu(E_\mu)$$

- $R_\mu = 2 \text{ km @ } 1 \text{ TeV}$
- $R_\mu = 10 \text{ km @ } 100 \text{ TeV}$
- $R_\mu^{\text{max}} = 50 \text{ km @ } 1 \text{ EeV}$

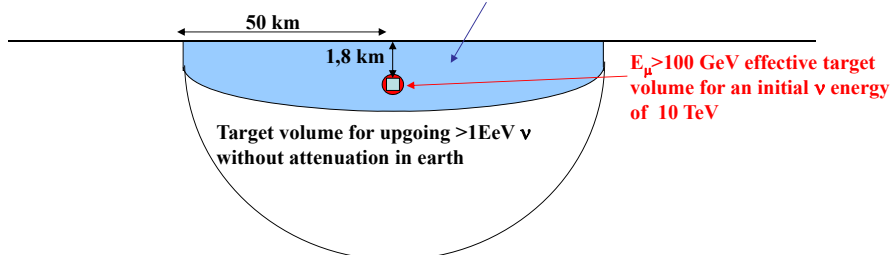
PeV ν_μ in IceCube



$$\frac{\partial \phi_1(E, z)}{\partial z} = -\frac{\partial P_{\text{loss}}^1(E, z)}{\partial z} \phi_1(E, z) + \sum_j \int_E^\infty \frac{\partial P_{j \rightarrow 1}^1(E', E, z)}{\partial E \partial z} \phi_j(E', z) dE'$$

$$\frac{dN_{\mu E > 1 \text{ PeV}}}{dE} = 2\pi \int_{-1}^1 \frac{\partial \phi_1(E, z(\cos \theta))}{\partial z} \sigma_{\text{cc}}(E) \frac{P_{\text{det}}}{m_p} \text{Min}(R_\mu, z(\cos \theta)) d(\cos \theta)$$

Target volume accounting for $E_\mu > 1 \text{ PeV}$ range and an ν initial energy of $1 \text{ EeV} \sim 10^{13}$ tons of ice.

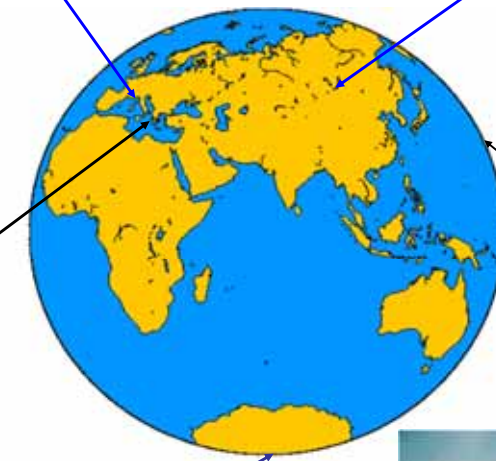


$E_\mu > 100 \text{ GeV}$ effective target volume for an initial ν energy of 10 TeV

Neutrino Telescope Projects

ANTARES La-Seyne-sur-Mer, France
 NEMO Catania, Italy, KM3NET ?

BAIKAL: Lake Baikal, Siberia



NESTOR : Pylos, Greece

DUMAND, Hawaii (cancelled 1995)

AMANDA, ICECUBE South Pole, Antarctica



AMANDA

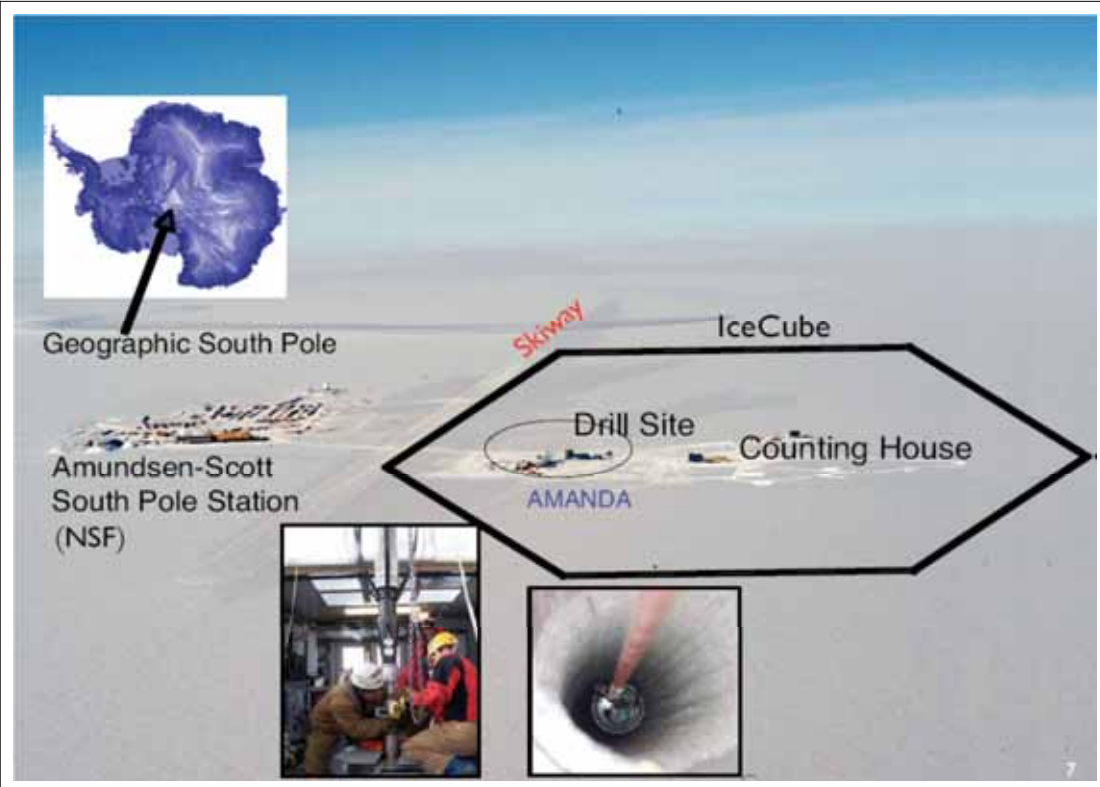
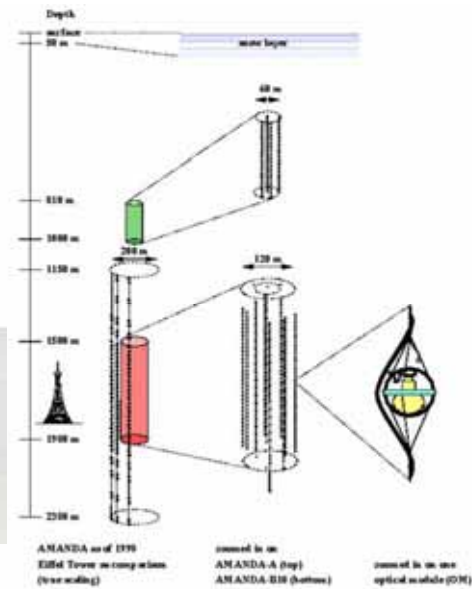
South Pole: glacial ice

- 1993 First strings AMANDA A
- 1998 AMANDA B10 ~ 300 Optical Modules
- 2000 ~ 700 Optical Modules
- ICECUBE 8000 Optical Modules

IMZR PSA - 2008-2009



AMANDA
 $\nu > 50\text{GeV}$



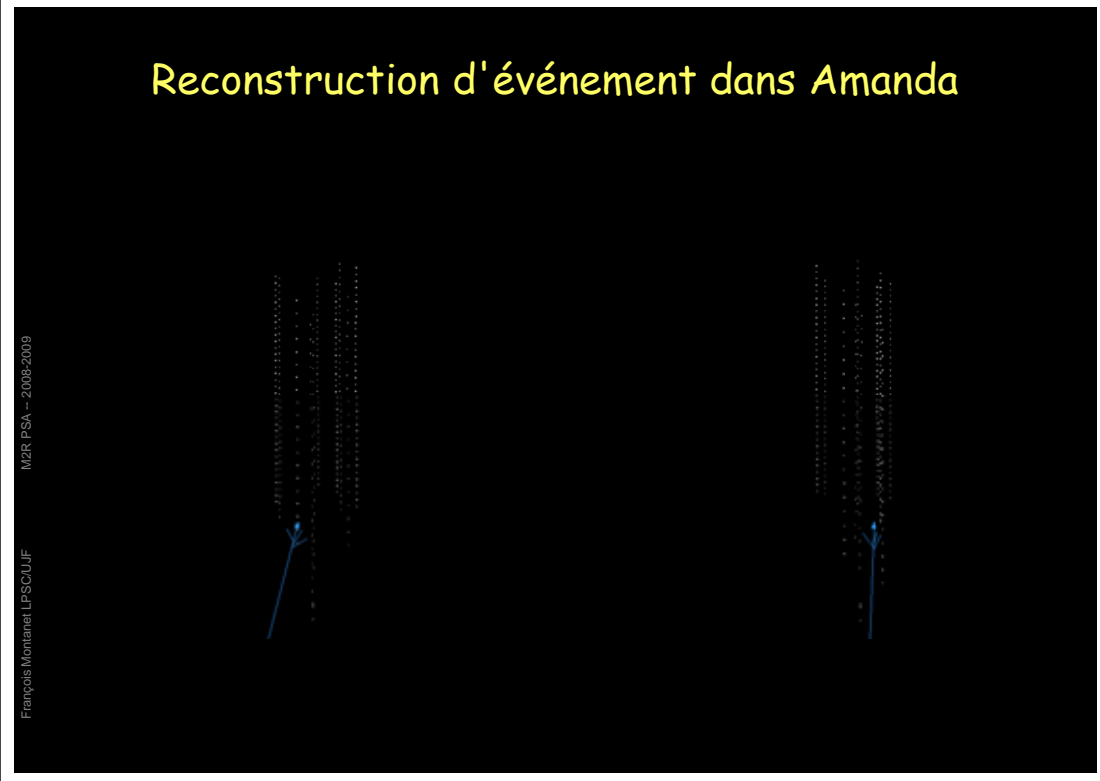
AMANDA: Drill Holes in ice with Hot Water

IMZR PSA - 2008-2009



Reconstruction d'événement dans Amanda

IMZR PSA - 2008-2009



The IceCube detector

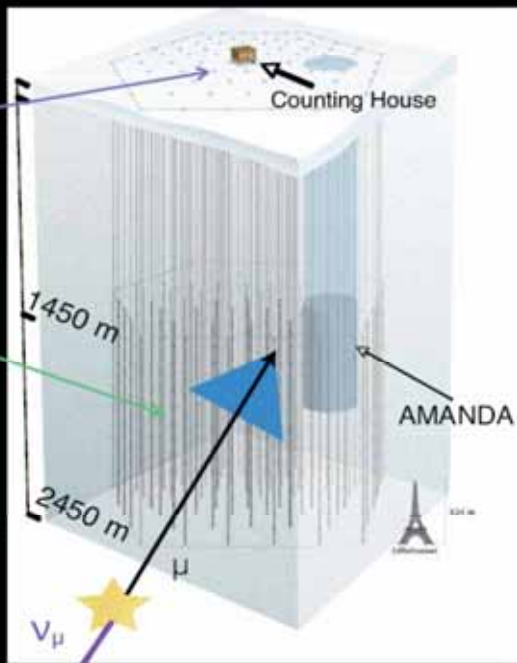
instrumenting 1 km³ of ice

IceTop :
Surface air shower array
Frozen tanks - 2DOMs

InIce :
80 strings each with 60 digital optical modules (DOM)

125m spacing between strings
17m between DOMs

Detect ν of all flavors
E range : 10¹¹ to 10²⁰ eV

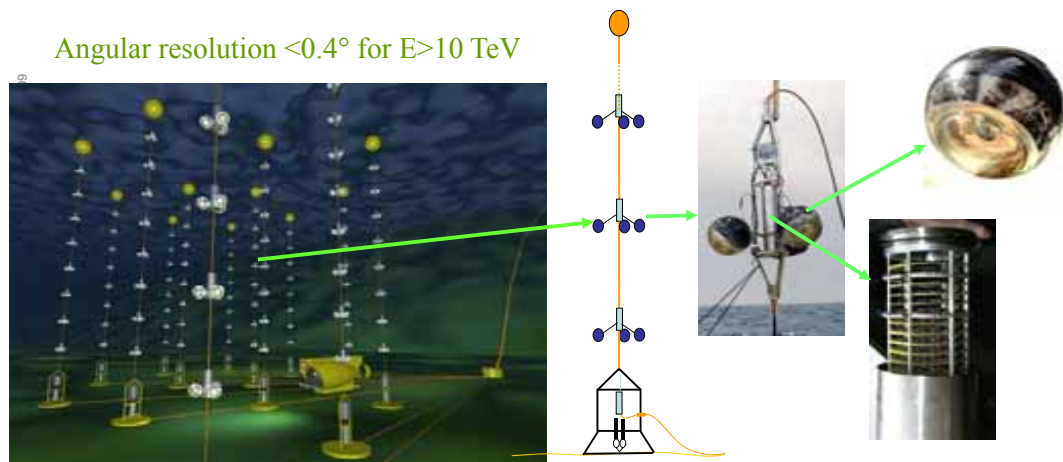


Future in ν telescopes: ANTARES

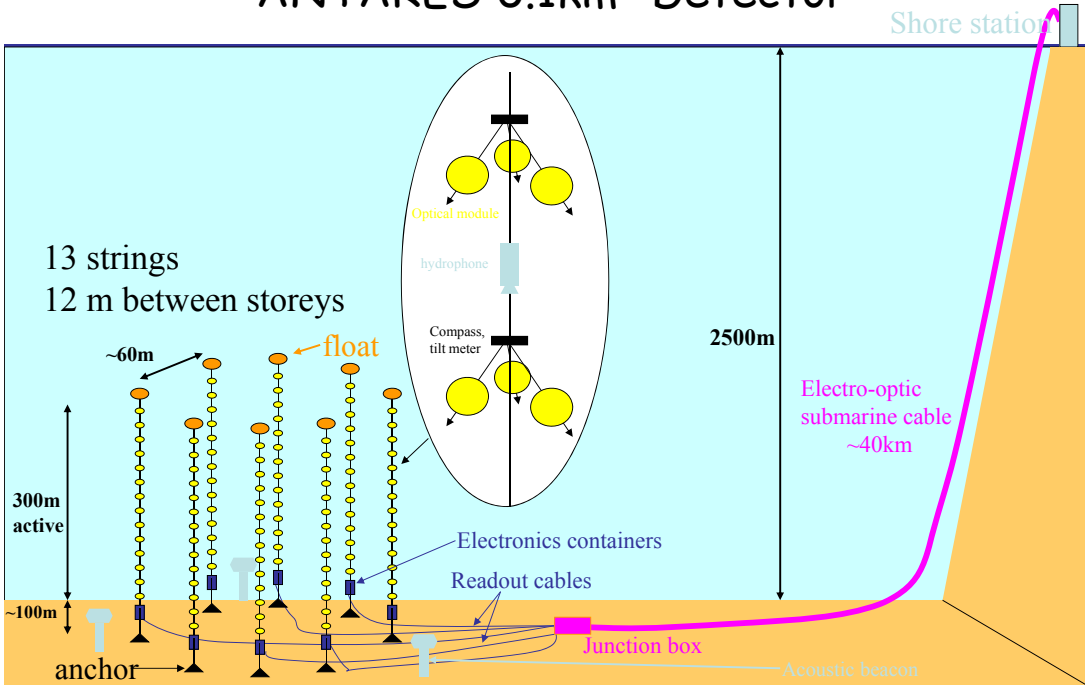


- 1996 Started
- 1996 - 2000 Site exploration and demonstrator line
- 2001 - 2004 Construction of 10 line detector, area ~0.1km² on Toulon site
- future 1 km³ in Mediterranean

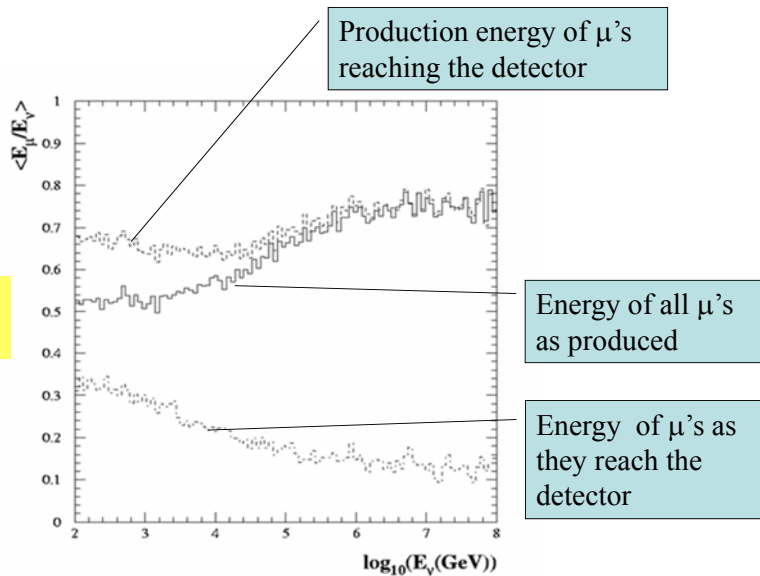
Angular resolution <0.4° for E>10 TeV



ANTARES 0.1km² Detector

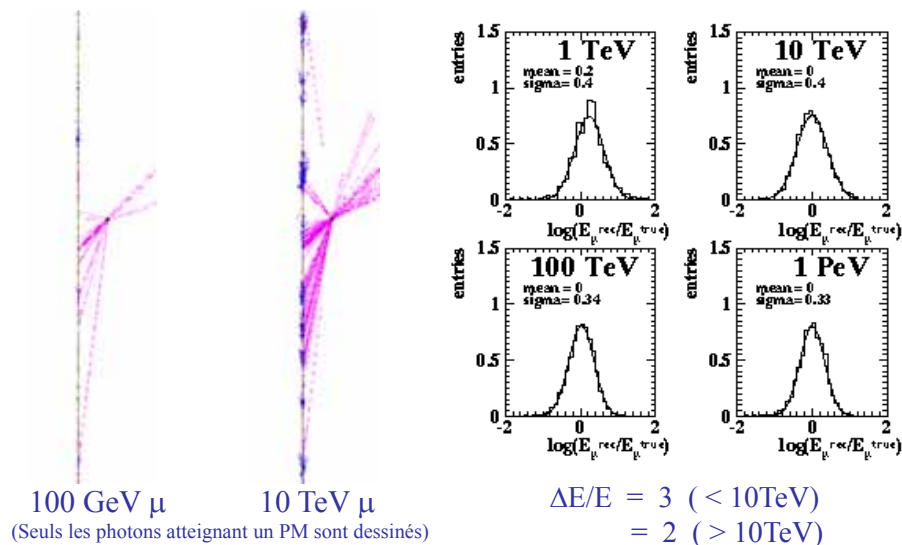


Principe de détection



Mean E_μ/E_ν ratio versus E_ν

Energy measurement



100 GeV μ 10 TeV μ
(Seuls les photons atteignant un PM sont dessinés)

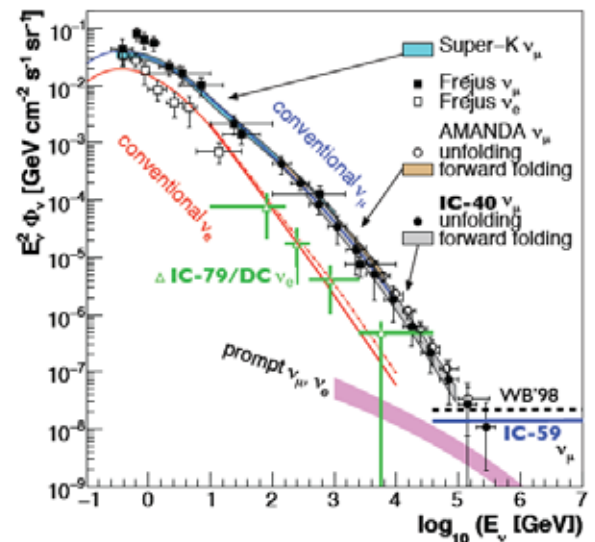
Il est possible de couper sur l'énergie du muon (par ex. à 1 PeV) et ainsi de rejeter les muons de neutrinos atmosphériques de basse énergie.

ν_μ	ν_e	ν_τ
<p>6×10^{15} eV (6 PeV) ~1000 DOMs hit ~ 20 km</p>	<p>$E = 375$ TeV "spherical" shell</p>	<p>$E = 10$ PeV 2 bangs separated by ~ $50 \cdot (E_\nu/\text{PeV})$</p>
<p>$E \sim dE/dx$, $e > 1$ TeV E res : $\Delta \log(E) \sim 0.3$ ang res : 0.8-2 deg</p>	<p>poor angular resolution E res : $\Delta \log(E) \sim 0.1-0.2$</p>	<p>very low background pointing capability good E measurement</p>

ICECUBE atmospheric flux

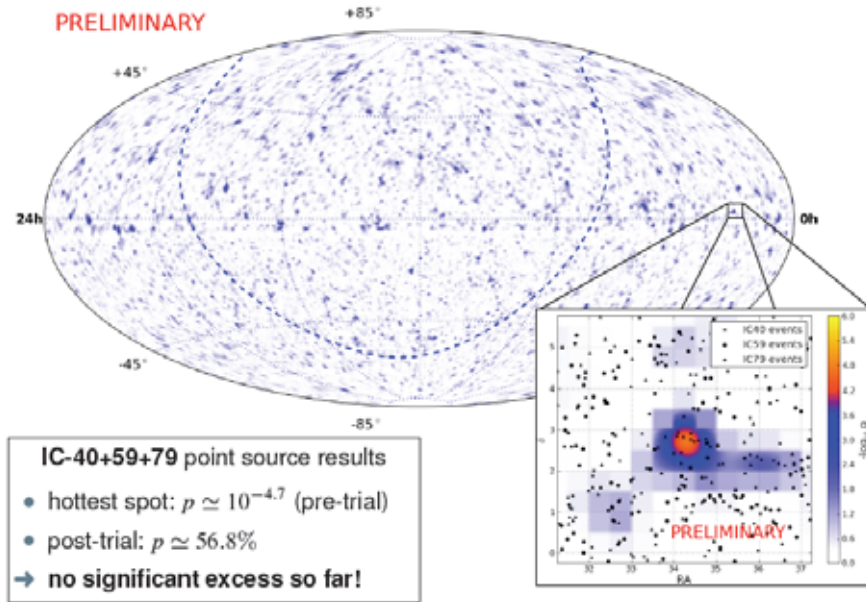
Atmospheric neutrino flux and diffuse limit

- high-energy atmospheric ν_μ/ν_e -spectrum as seen by IC-40 & IC-79/DC [IceCube'11,'12]
- diffuse ν_μ limit from IC-59 (90% C.L.) (preliminary)
- predicted prompt atmospheric ν -fluxes (charmed meson decay) [Enberg et al.'08]
- theoretical limit on diffuse astrophysical ν_μ 's [Waxman&Bahcall '98]



ICECUBE atmospheric flux

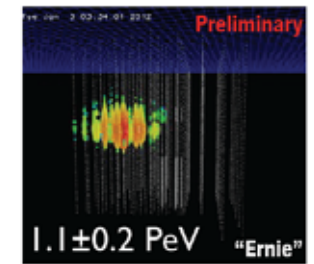
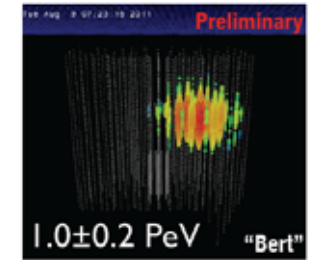
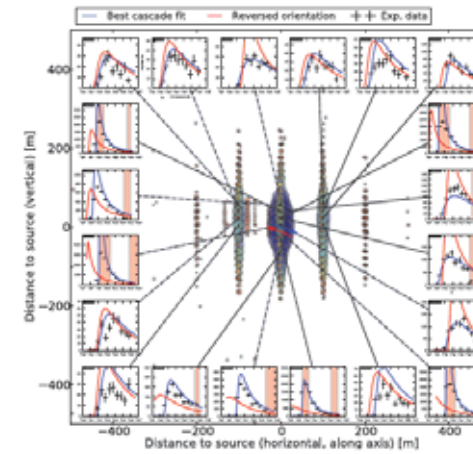
Steady point-source search



ICECUBE atmospheric flux

Extremely-high energy analysis

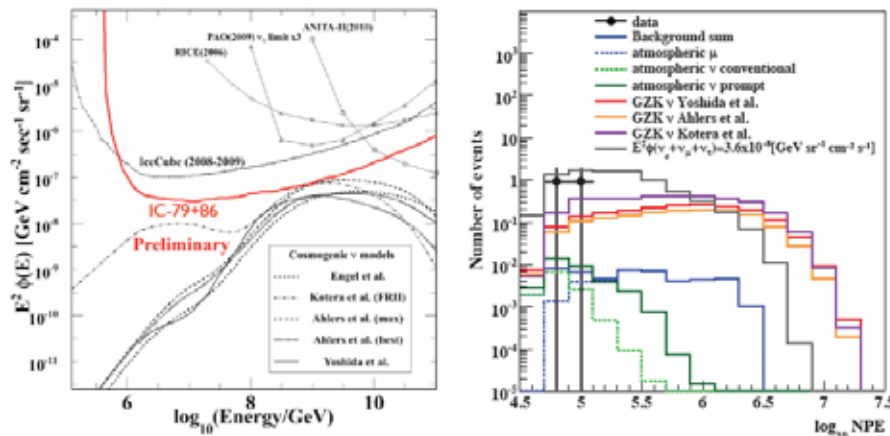
Follow-up studies of background events:
energy, orientation,...
 → Are there more contained events?



ICECUBE atmospheric flux

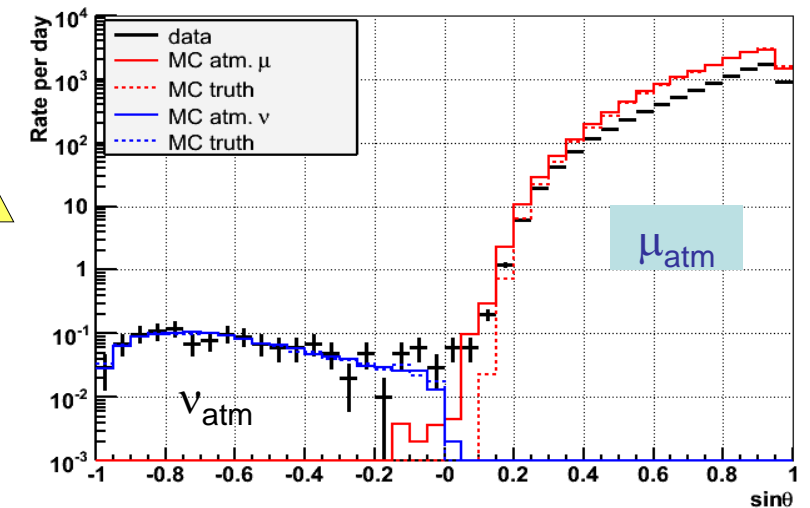
Extremely-high energy analysis

- Study for cosmogenic neutrino fluxes in IC-79+86
- optimized cuts on zenith angle and "brightness" (NPE: number of photo-electrons)
- two "background" events above NPE threshold

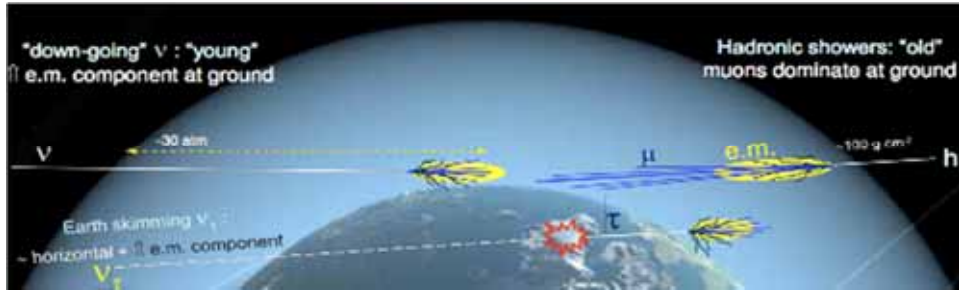


Premiers résultats d'Antares 12 lignes (sur 120 jours actifs)

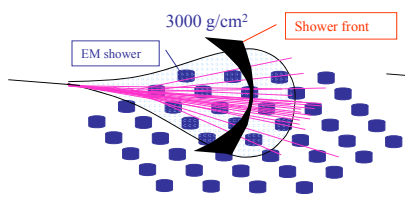
Elevation



Neutrinos UHE : Gerbes Horizontales

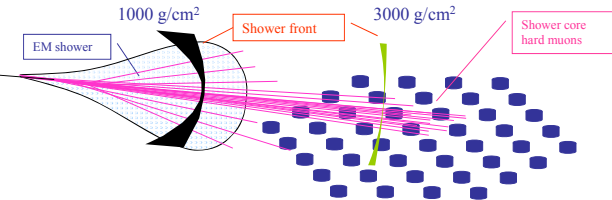


ν : "new" showers



Signal is:
 Few events per year
 EM rich, curved and thick front
 Broad signals

hadrons: "old" showers



Background is:
 Thousands events per year
 EM poor, muon rich, flat and thin front
 Prompt signal

AUGER limits

